Electron-impact excitation of the sodium atom

James O. Phelps and Chun C. Lin
Department of Physics, University of Wisconsin, Madison, Wisconsin 53706
(Received 19 February 1981)

Absolute electron-impact optical-excitation functions of 26 transitions of the sharp, principal, diffuse, fundamental, and nP-$4S$ series of sodium have been measured in the impact-energy range 0–150 eV. The determination of the target-atom number density was made by measuring the attenuation of sodium resonance radiation from a fluorescence cell upon passage through the collision chamber. Direct-excitation cross sections of 14 states ($4S$, $5S$, $6S$, $7S$, $3P$, $4P$, $5P$, $6P$, $3D$, $4D$, $5D$, $6D$, $6F$, and $7F$) have been determined from the measured optical-excitation cross sections with the aid of radiative-transition probabilities taken from the literature. These direct-cross-section results are compared with theoretical calculations based upon the Born approximation and the multistate-close-coupling approximation. Measurements were also made of the polarization of several sharp, principal, and diffuse series-resolved doublets, and from these results the direct-excitation functions of the separate orbital magnetic sublevels of the $3P$ state have been determined.

I. INTRODUCTION

Electron-impact excitation of the sodium atom has been the subject of experimental and theoretical investigations since the 1930's. The work prior to 1968 has been reviewed by Moiseiwitsch and Smith,[1] while that done between 1968 and 1977 has been covered by Bransden and McDowell.[2] Despite the amount of attention the problem has received, the available body of experimental excitation-cross-section data remains to a great extent incomplete and contradictory. The excitation of certain states has never been measured, and for many other states the observations do not extend beyond 30 eV. Among those cases where more than one measurement of a cross section has been reported, discrepancies amounting to a factor of 2 or more are common. Even in the most extensively studied case, i.e., the excitation of the $3P$-$3S$ transition, the most recently reported peak cross sections differ by 50%, while the quoted margins of error are only 6–8%.[3,4] The most likely sources of such discrepancies, as inferred from the individual experimental descriptions, include determination of the atom number density, scattering of resonance radiation, contamination of the electron beam by secondary electrons, problems with the radiometric calibration, particularly in the uv, window degradation by chemical attack, and problems in coupling the photodetection optics with the electron beam (as well as with the atomic beam, in crossed-beam experiments). It is to the solution or at least amelioration of these and other technical problems, all of which have been identified and understood for some time, that we have given first priority in our experiment. With these improvements and with the enhanced photodetection capabilities of the past decade, we have sought to obtain a unified body of excitation-cross-section measurements that is more comprehensive, in terms of the number of excited states (see Fig. 1) and the range of impact energies investigated, and of greater reliability and precision than has previously been available. The new experimental data are then compared with theoretical calculations based on the Born approximation and the method of close coupling.

This experiment represents a continuation of our earlier work on electron-impact excitation of potassium,[5] with which frequent comparisons will be made in the present report.

II. EXPERIMENTAL PROCEDURE

A detailed description of the experimental apparatus and procedure has been given in our po-

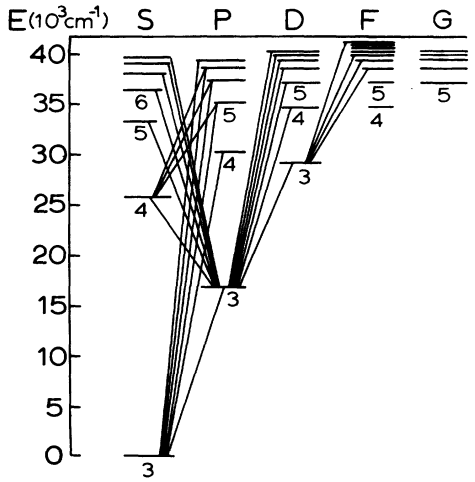

FIG. 1. Energy levels of sodium. The transitions observed in the present experiment are indicated by lines joining the levels.

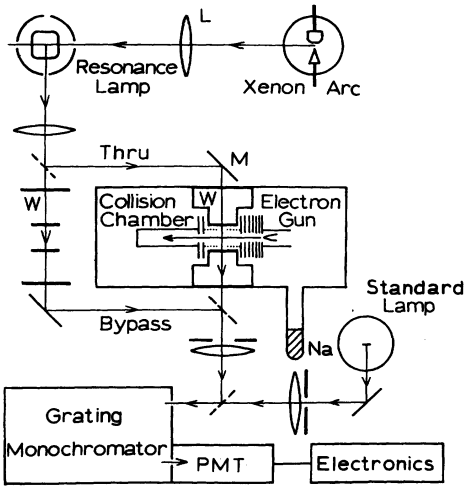

FIG. 2. Schematic diagram of apparatus. Lenses are denoted by the usual symbol, such as the one marked "L". Mirrors are indicated by diagonal lines, like the one marked "M," solid if fixed, dashed if removable. "Thru" and "Bypass" identify the two alternative paths for resonance radiation from the resonance lamp (i.e., fluorescence cell). The collision chamber windows and compensating windows are indicated by a "W."

tassium paper and will not be repeated here. Few of the experimental specifications needed to be changed for the present work. Thus, we limit our present discussion to a review of the experiment and to a description of the modifications made and special precautions taken.

The apparatus is diagrammed in Fig. 2. Sodium is evaporated from a sidearm into an evacuated, heated collision chamber. A monoenergetic (<0.75-eV FWHM) beam of electrons (2–25 μA) passes through and excites the vapor, and the subsequent radiative decay is observed at right angles to the electron beam. The various spectral lines are selected by a grating spectrometer and detected by a photomultiplier, the output of which is measured by either a photon counter or an electrometer. Radiometric calibration of the detection system is done by comparison against a standard source, either a tungsten strip lamp or a tungsten-quartz-halogen lamp. The atom number density in the collision region is determined by measuring the degree of attenuation of sodium resonance radiation as it passes through the collision chamber, the source of this radiation being a sodium resonance lamp or fluorescence cell, excited by continuum radiation from a xenon arc.

The sidearm temperature was varied between 120 and 210 °C, producing number densities in the range 2×10^{10} to 4×10^{12} atoms/cm^3. As in our potassium experiment, the collision chamber was continually pumped through a high impedance. Since the effective area of this exhaust orifice, a few mm^2, was much smaller than that of the vapor source, i.e., the molten sodium, its presence did not greatly reduce the steady-state Na vapor pressure; yet it allowed sufficient pumping speed to prevent the accumulation of unacceptable levels of foreign gases in the collision chamber due to leakage or outgassing. Such impurities were readily detected by measuring the intensity of prominent lines of the electron-impact radiation. In particular, to test for N_2 we looked for the first negative band of N_2^+ at 3914 Å, which has a large, accurately known excitation cross section.[6] The intensity we observed for this band was generally negligible or very weak, putting an upper limit of 2×10^{10} molecules/cm^3 on the density of N_2. A similar search for the Hα line of atomic hydrogen, which we have found to be a sensitive indicator of the outgassing of H_2O into systems containing hot alkalis, was negative. The most abundant contaminant found was potassium, which was continually evolving from the walls, where it had evidently been absorbed during our previous experiment. From measurements of the K $D1$ line intensity we found the K density to be approximately 5×10^{10} atoms/cm^3. These various impurities did not interfere with the Na spectrum or with other aspects of the experiment and were therefore tolerated.

For practical reasons the operating temperature of the collision chamber was restricted to a fairly narrow range about 275 °C. Thus we did not investigate the dependence, if any, of the excitation signal upon the collision chamber temperature. The possibility of such a dependence, caused by interaction of the excited atoms with the blackbody radiation field, will be discussed in our error analysis, Sec. III B.

Sodium proved to be more difficult to work with than potassium in several ways—the copper braze of the sapphire-to-kovar window seals was attacked, the uv transmittance of the windows was degraded and had to be continuously monitored, and the electrical insulation of the electron-gun feedthroughs deteriorated. Consequently, lower number densities had to be used, and this, in conjunction with the generally smaller cross sections of sodium (versus potassium) and the narrower spectrometer slit width required to separate the more closely spaced doublet structure of the sodium spectrum, resulted in weaker experimental signals. These factors limited the number of lines we were able to study and restricted the maximum impact energy to 150 eV. For the weaker signals, the electrometer measuring the photomultiplier output was replaced by a photon-counting system.

In general, electron-impact radiation is emitted anisotropically. We wish to determine the total radiation into all directions from measurements made at a single angle, 90° from the electron beam. It is possible to do this since the total intensity, integrated over all angles, is proportional to $I_{\parallel}+2I_{\perp}$, where $I_{\parallel}$ and $I_{\perp}$ are the intensities of the components of light emitted 90° to the electron beam, with electric vector parallel to and perpendicular to the electron beam, respectively.[1] Thus a detection system at 90° that responds simultaneously to both polarizations with efficiencies in the ratio $\epsilon_{\perp}/\epsilon_{\parallel}=2$ will produce an output that is proportional to the angle-integrated intensity, i.e., to the total rate of the radiative transition. This efficiency ratio can be obtained at the expense of signal strength by inserting a polarizing filter in the light path, oriented with its electric vector transmission axis at the "magic angle," $\theta_m=\arctan\sqrt{2}=54.7°$, relative to the electron beam.[1] This was done for a number of lines, specifically the first few members of the principal and diffuse series. For the upper members of these series and for all observed members of the fundamental series, no polarizer was used on account of signal weakness. In the case of the upper principal series, indications are that the polarization is rather weak (see Sec. V), in which case the emission is nearly isotropic and no polarizer is necessary. For the upper diffuse series, the grating efficiency favors $I_{\perp}$ over $I_{\parallel}$ by about 1.7:1, which, while not identical to the ideal 2:1, should produce a signal nearly proportional to the angle-integrated intensity. For the entire sharp series the emission is isotropic and therefore no correction is needed.[1] Thus, it is only for the fundamental series that the observed intensity may differ appreciably from the total emission. At the wavelengths of the lowest three observed lines the instrumental polarization is small, so the angle-averaged intensity is obtained from the observed intensity by multiplication by the well-known[1] polarization correction factor $(1-P/3)$, where P is the polarization of the emission at 90° given by $(I_{\parallel}-I_{\perp})/(I_{\parallel}+I_{\perp})$. We do not have a measurement of P so this correction is not applied. Using the diffuse series as a guide (Sec. V) we might estimate P at 15 eV to be about 0.2, in which case the angle-averaged intensity for the fundamental series at this energy would be about 7% lower than the observed intensity.

The spectrometer slit width was kept constant throughout the experiment; the full width at half maximum (FWHM) of the passband was approximately 5 Å, except for wavelengths beyond 9000 Å, where use of a coarser grating gave a passband of 10 Å. This was sufficient to resolve the $3P$ spin-orbit splitting and hence, the doublet structure of the $3P$-$3S$ transition and of the entire sharp and diffuse series. The 2:1 intensity ratio of the two components of all these doublets was verified at an impact energy of 15 eV. In view of this simple proportionality, we carried out our definitive cross-section measurements for just one of the components of each doublet, then multiplied by the appropriate statistical factor to obtain the cross section for the combined doublet.

A. Radiometric calibration

The spectrum of sodium extends farther into the ultraviolet than does that of potassium, the principal series limit being 2412 Å. For these wavelengths the tungsten strip lamp that had been used as the radiometric standard in our potassium experiment was unsuitable on account of the low uv radiance of the tungsten ribbon at its maximum operating temperature 2000 K, and because of absorption by its Pyrex window. Instead, for wavelengths below 3400 Å, we used a freshly calibrated Optronics Model 245-C tungsten-quartz-iodine spectral irradiance standard lamp[7] operating at an effective temperature of about 2920 K. (When this lamp is used, the lens and aperture stop indicated in the standard-lamp light path in Fig. 2 are removed.) The precision of the calibration of this lamp, traceable to NBS, is 3%. In the range where both the strip lamp and the tungsten-quartz-iodine lamp could be used, i.e., above about 3400 Å, the two were found to be in excellent agreement (2%). In practice we found the strip lamp to be preferrable at these longer wavelengths because of the excessive brilliance of the tungsten-quartz-halogen lamp in the visible and infrared.

In carrying out the uv radiometric calibration of our system we took extensive precautions to ensure adequate monochromatization of the light from the standard lamp. Because of the susceptibility of uv calibration to very large systematic errors, we discuss these precautions in detail. The principal difficulty in using incandescent standard lamps arises from the weakness of their output in the uv relative to the visible and infrared (ir). As a worst-case example, we consider the shortest wavelength of our experiment, 2544 Å, which corresponds to the $8P$-$3S$ transition. At this wavelength only one photon in about 2×10^6 of the lamp's continuum spectrum (weighted by the quantum efficiency of the GaAs photocathode) occurs in the desired 5-Å passband of the monochromator. The remainder are a source of stray light at the exit slit, due to scat-

tering within the spectrometer by dirty or imperfect optics or mountings, or due to grating ghosts or multiple dispersion paths. The stray light produces spuriously large standard-lamp signals, and if not removed or corrected for, leads to erroneously small values for uv excitation cross sections. Of the unwanted portion of the standard-lamp's emission, 98–99% was removed before reaching the spectrometer by a Corion "solar-blind" filter,[8] having an irregularly shaped passband from 2400 to 3600 Å and a peak transmittance of 80% (it also has a weak, <5%, transmission band beyond 7500 Å). A similar, alternative filter made in our laboratory consists of a 12-mm path through an aqueous solution of 1.4*M* $NiSO_4$ plus 0.4*M* $CoSO_4$, with end windows of Corning glass 9863, 1 mm thick.[9-11]

In the monochromator we used a new uv-blazed grating having particularly low light scatter. We had the mirror freshly re-aluminized and installed additional high-absorbance baffling to intercept the zeroth-order diffracted beam. The light from the standard lamp was in a small cone so there was no scattering from nonoptical surfaces. Each of these measures was effective in reducing the stray light.

Several tests were run to detect spectral impurities. One of these involves the use of an auxiliary filter, such as Corning 7-54, having a strongly varying transmittance in the uv. If a monochromator with poor stray light rejection is used to measure the transmittance of such a filter, then different values for the apparent transmittance will be indicated when sources of different spectral distributions, or detectors with different spectral sensitivities are used. We tried three different sources (the tungsten-quartz-halogen lamp producing a smooth continuum increasing rapidly in intensity toward longer wavelengths, a deuterium lamp with a continuum increasing in intensity toward shorter wavelengths, and a low pressure mercury discharge giving an atomic line spectrum) and two different detectors (the GaAs photocathode and a bialkali photocathode having a stronger uv response and no ir response). These yielded the same transmittance values provided the tungsten-quartz-iodine lamp was filtered through the solar-blind filter as described. In another test we used relatively sharp-cut, high-wavelength-pass colored glass filters to determine roughly the spectral distribution of the standard-lamp scattered light[12] with the spectrometer tuned to 2544 Å. To estimate the distribution on a finer scale, i.e., within 300 Å of the nominal uv wavelength, we determined approximately the wings of the instrumental function by making scans of nearby intense mercury lines, and then integrated this function against the spectral intensity of the filtered standard lamp. In further tests we analyzed the output of the monochromator with an auxiliary spectrometer and determined the locations and strengths of grating ghosts. Calculations were also made of multiple-dispersion paths,[13] but for the configuration of our monochromator (0.5-m Ebert) and with the incident light confined to the vicinity of the optic axis no troublesome paths were found involving wavelengths that were not blocked by the solar-blind filter. Finally, subsequent to the experiment proper, we compared our tungsten-quartz-iodine lamp with a recently acquired Optronics Model uv-40 deuterium standard lamp. The radiometric calibration of our system obtained from these two different standard lamps are in agreement within the 10% uncertainty assigned by NBS to the deuterium lamp's original calibration; the sign of the discrepancy between the two sources is opposite to that which would result if the tungsten-quartz-halogen lamp contained a stray light component.

These various tests established conclusively that even in the most extreme case spectral impurities did not contribute as much as 5% of the standard-lamp signal; at longer wavelengths stray light became completely negligible. Thus, this frequently dominant source of error is reduced to the level of such other factors as lamp current measurement and stability (10^{-4} A), wavelength accuracy (0.3 Å), photomultiplier linearity, geometrical measurements, original NBS calibration, and its transfer by the lamp supplier, etc. We estimate the resultant uncertainty in our radiometric calibration due to these sources to vary from an optimum of 7% in the visible to a maximum of 12% in the uv limit.

B. Determination of atom number density

To determine the number density we used the resonance-line transmission method described in our potassium paper.[5] With sodium, even more than potassium, this technique offers significant advantage over such alternative methods as surface ionization or the use of standard vapor pressure tables. With the former method, there is the problem of uncertainty in the ionization efficiency. With the latter method the problems of establishing thermodynamic equilibrium and the discrepancies among published vapor pressure tables are more serious for sodium than potassium. For example, at a typical evaporation temperature used in sodium electron-impact studies, 160 °C, the most recent comprehensive critical evaluation by Hultgren *et al.*[14] indicates

a vapor pressure approximately 50% higher than the standard tables[15] used by previous electron-impact experimenters.[16,17]

The computation of the transmittance $T(NL)$ of the vapor layer in the collision chamber, of density N, thickness L, for the sodium $D1$ line $3P_{1/2}$-$3S_{1/2}$ is carried out in the same way as for the analogous potassium line.[5] The values of the relevant parameters are as follows. Sodium has only one stable isotope, $A=23$, with a nuclear spin $I=3/2$. Thus the possible values for the total angular momentum (electronic plus nuclear) are $F'=1,2$ for the upper state ($3P_{1/2}$) and $F=1,2$ for the lower state ($3S_{1/2}$). With f denoting the oscillator strength of the entire $D1$ transition, the absorption oscillator strengths of the four hyperfine components $f_{FF'}$ are given by $f_{11}=f/6$, $f_{12}=5f/6$, $f_{21}=f_{22}=f/2$, just as for potassium. The value of f is 0.327, with a precision of 3%.[18] The displacements of these components from the overall line centroid, $\bar{\nu}_{FF'}$, in units of 10^{-3} cm^{-1}, are $\bar{\nu}_{11}=33.0$, $\bar{\nu}_{21}=-26.1$, $\bar{\nu}_{12}=39.3$, and $\bar{\nu}_{22}=-19.8$.[19] The probability W_F of a ground-state atom having a given initial value of F should be proportional to the statistical weight $2F+1$, so the two probabilities are $W_1=\frac{3}{8}$ and $W_2=\frac{5}{8}$. The hyperfine splitting of the ground state and the Doppler width (FWHM at 275 °C) are, by coincidence, virtually identical, 59.1×10^{-3} and 59.2×10^{-3} cm^{-1}, respectively, so that the $D1$ line has two distinct maxima. The natural width of the line is $\Gamma=0.334\times10^{-3}$ cm^{-1}, FWHM.[18] Using these parametric values we computed the normalized Voigt profiles $U_{FF'}(\bar{\nu})$ of the separate hyperfine components, then formed the overall resonance absorption cross section $K(\bar{\nu})$ of the $D1$ line by taking the weighted sum

$$K(\bar{\nu})=\sum_F\sum_{F'}\pi r_e W_F f_{FF'}U_{FF'}(\bar{\nu}), \qquad (1)$$

where r_e is the classical electron radius. [We would like to point out that in the corresponding equation in our potassium paper, Eq. (6) of Ref. 5, the factor W_F is missing by typographical error.]

The emission profile $I(\bar{\nu})$ of the fluorescence cell, excited by white light from the xenon arc, is calculated in the same way but with the substitution of the cell temperature 125 °C.

From these absorption and emission profiles the integrated transmittance $T(NL)$ of the vapor in the collision chamber is calculated as a function of vapor density, with the result shown in Fig. 3. Use of this curve permits determination of the number density N from experimental measurements of the transmittance T and the geometrical path length L within the collision chamber, this

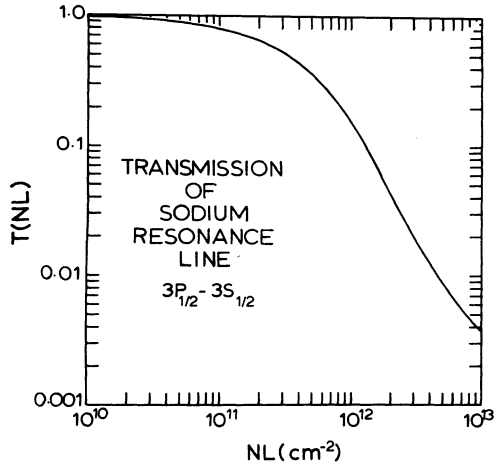

FIG. 3. Calculated integrated transmittance $T(NL)$ of the sodium $D1$ line. The source is resonance fluorescence from an optically thin vapor at 125 °C excited by white light. The absorber is a layer of NL sodium atoms/cm^2 at 275 °C.

latter value being fixed at 1.43 cm throughout the experiment. In practice several minor refinements were made in the calculation of $T(NL)$ pertaining to the attenuation and reflection, within the fluorescence cell, of both the exciting light from the xenon arc and the sodium fluorescence. At an operating temperature of 125 °C the vapor density in the cell, as determined from a standard vapor pressure reference,[14] is 3.3×10^{10} atoms/cm^3 (or less according to alternative tabulations). The peak value of the Na $D1$ absorption cross section is computed to be 3.34×10^{-12} cm^2, while the distance between the center and the wall of the square fluorescence cell is 0.50 cm; hence, the maximum optical depth of the source, the product of the above, is 0.056. The effect of this small departure from ideal optical thinness is that the profile of the emergent fluorescence is slightly broadened—partially because of self-absorption of the fluorescence and partially because the frequency dependence of the attenuation of the exciting continuum radiation as it enters the cell causes a deviation from perfect "whiteness," which, in turn, alters the relative intensities of the various hyperfine components of the fluorescence. Both effects are slightly enhanced by reflections from the Pyrex cell walls since the reflected light traverses an additional layer of vapor. The net result of the inclusion of these effects is to increase the calculated transmittance through the collision chamber by a small amount, no more than 0.002, which translates into a very small increase in the value deduced for the number density. A more problematic aspect of the transmittance measurements is that of multiple

TABLE I. Experimental optical-excitation functions of sodium.

Transition $j \rightarrow k$	Wavelength (Å)	Uncertainty[a] (%)	Optical-excitation cross section Q_{jk} (10^{-18} cm^2) at E (eV) 5	7	10	15	20	30	50	75[b]	100[b]	150[b]
$4S$-$3P$	11 382–11 404	20	251	223	203	187	174	150	115	86.0	71.2	(48.0)
$5S$-$3P$	6154–6161	10	30.5	24.3	21.2	20.1	19.4	16.7	12.8	9.45	7.56	5.09
$6S$-$3P$	5159–5153	12	9.32	6.91	5.29	5.14	5.07	4.56	3.58	2.75	2.03	1.39
$7S$-$3P$	4748–4752	12	2.65	2.74	2.18	2.05	2.08	1.86	1.53	1.10	0.82	0.57
$8S$-$3P$	4542–4545	12	0.58	1.46	0.96	1.01	1.04	0.98	0.76	(0.55)	(0.45)	(0.28)
$9S$-$3P$	4420–4423	15	0.19	0.66	0.49	0.51	0.54	0.52	0.42	(0.30)	(0.23)	(0.16)
$3P$-$3S$	5890–5896	10	4290	4450	4340	4050	3740	3190	2530	1940	1560	1130
$4P$-$3S$	3302–3303	15	40.8	40.7	38.8	36.6	33.6	28.0	20.8	14.7	11.5	7.87
$5P$-$3S$	2853	20	5.68	6.37	5.70	5.62	5.24	4.61	3.36	2.45	1.92	1.38
$6P$-$3S$	2680	20	1.31	1.79	1.53	1.47	1.47	1.32	0.97	(0.70)	(0.55)	(0.40)
$7P$-$3S$	2594	20	0.37	0.59	0.51	0.52	0.52	0.46	0.35	(0.26)	(0.20)	(0.15)
$8P$-$3S$	2544	25	0.16	0.28	0.22	0.21	0.21	0.21	0.17	(0.12)	(0.09)	(0.07)
$3D$-$3P$	8183–8195	10	443	489	444	354	290	209	134	86.4	64.8	41.8
$4D$-$3P$	5683–5688	10	38.5	67.5	65.8	54.1	44.3	33.0	21.5	14.7	11.1	7.25
$5D$-$3P$	4978–4983	12	15.0	20.5	20.6	17.8	15.0	11.3	7.53	5.15	3.67	2.46
$6D$-$3P$	4665–4669	12	4.30	8.53	8.84	7.91	6.95	5.12	3.45	2.25	1.68	1.04
$7D$-$3P$	4494–4498	12	1.78	4.19	4.35	4.10	3.61	2.80	1.91	1.27	0.94	0.59
$8D$-$3P$	4390–4393	12	0.46	2.31	2.34	2.24	2.02	1.64	1.10	(0.73)	(0.54)	(0.34)
$9D$-$3P$	4321–4325	15	0.13	1.32	1.33	1.29	1.18	0.95	0.67	(0.45)	(0.33)	(0.21)
$6F$-$3D$	10835	20				5.03						
$7F$-$3D$	9961	20				2.47						
$8F$-$3D$	9466	25				1.49						
$12F$-$3D$	8684	25				0.21						
$5P$-$4S$	10 746–10 749	20	8.75	9.82	8.78	8.66	8.07	7.10	5.18	3.75	2.96	2.13
$6P$-$4S$	8650	20	1.69	2.31	1.98	1.90	1.90	1.71	1.25	(0.90)	(0.71)	(0.52)
$7P$-$4S$	7810	20	0.48	0.77	0.67	0.68	0.68	0.60	0.46	(0.34)	(0.26)	(0.20)

[a] Uncertainties correspond to 70% confidence level.

[b] Values in parentheses are based upon extrapolation.

reflections among the various collision chamber windows (two inner windows of sapphire, two outer of fused quartz) and among the corresponding compensating windows. Moreover, the sapphire windows, on account of their high refractive index and surface parallelism, are quite reflective and exhibit an annoying internal etalon effect with a free spectral range of about 1 Å. Care was taken to reduce these effects, but they did contribute a residual uncertainty of several percent to the deduced value of N. Combining this with other components, namely, uncertainty in the Na $D1$ oscillator strength and noise in the fluorescence signal, we estimate the precision of N to vary from 5–10% for densities in the range 3×10^{10} to 3×10^{12} atoms/cm^3. At lower densities the dependence of N on the measured transmittance is too sensitive, while at higher densities multiple scattering and line wing effects become non-negligible, leading to a degradation of the precision of N.

Several of the larger cross sections, i.e., those for the transitions $5S$-$3P$, $3P$-$3S$, $4P$-$3S$, $3D$-$3P$, and $4D$-$3P$ were measured at several number densities over the broad range 3×10^{10} to 4×10^{12} cm^{-3}, and many of the remaining lines were measured in the more restricted range 1×10^{12} to 4×10^{12} cm^{-3}. Except in the cases of $3P$-$3S$ and $4P$-$3S$, which are resonance lines, no systematic departure from direct proportionality between signal and number density was found, indicating the relative unimportance of nonlinear (with respect to density) processes, such as the quenching of excited atoms by collisions with ground-state atoms. However, for some of the smaller cross sections, particularly those originating in high-lying levels, our measurements were made at just one, comparatively high density, and for these the possibility of nonlinear effects cannot be excluded. This matter will be taken up in our error analysis.

At the densities used in this experiment the sodium dimer concentration should be less than 1%, according to the data summarized by Nesmeyanov.[20] Thus we do not consider any effects of Na_2 molecules.

III. EXPERIMENTAL RESULTS FOR OPTICAL-EXCITATION FUNCTIONS

A. General features

The fundamental quantities measured in this experiment are the optical-excitation functions $Q_{jk}(E)$, defined as the cross sections for production of $j \rightarrow k$ radiative transitions by impact of electrons of energy E upon atoms initially in the ground state. The compound process to which the cross section applies includes radiation into an entire sphere; it also includes both of the principal mechanisms of excited-state population, namely, direct excitation by electron impact and indirect excitation by radiative cascade from higher-lying excited states. Our measurements cover the 26 transitions between nL terms indicated in Fig. 1. These comprise the first six or seven doublets of the sharp (nS-$3P$), principal (nP-$3S$), and diffuse (nD-$3P$) series, and several members each of the fundamental (nF-$3D$) series

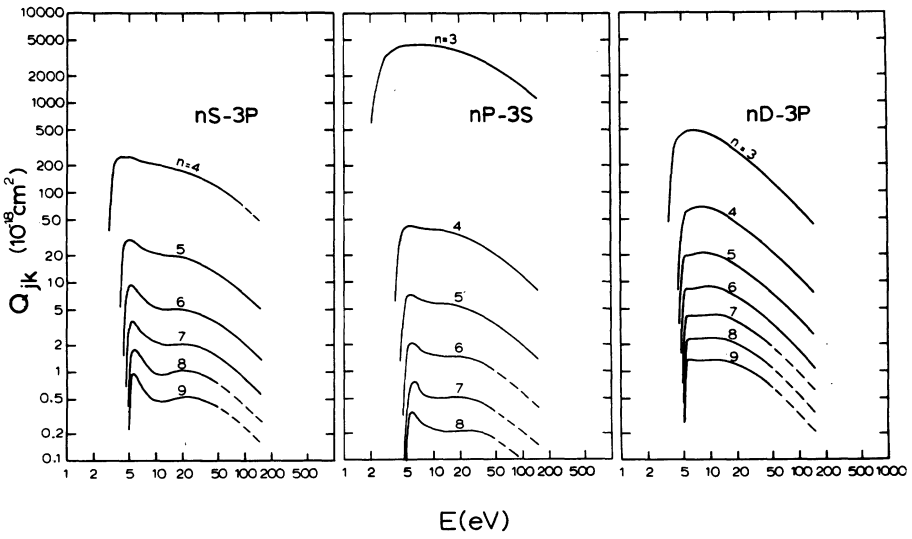

FIG. 4. Experimental optical-excitation functions of sodium for the sharp, principal, and diffuse series. Solid lines denote direct experimental measurements; dashed lines represent extrapolations with respect to energy, as explained in text.

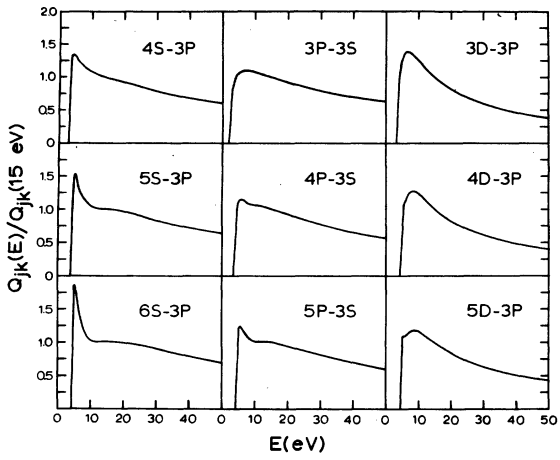

FIG. 5. Relative optical-excitation functions of the first three members of the sharp, principal, and diffuse series, scaled to unity at 15 eV.

and the nP-$4S$ series. Our results for all observed transitions are tabulated at selected impact energies in Table I. For the sharp, principal, and diffuse series a graphical display is also given, using a log-log scale, in Fig. 4. For purposes of shape comparison we have also plotted the first three members of each of these three series on a linear scale, normalized to unity at 15 eV, in Fig. 5.

For the sharp, principal, and diffuse series, the cross sections giving the stronger signals have been measured at impact energies up to 150 eV, and the others just to 50 or 100 eV. In each of the latter cases, each excitation function was then extrapolated to 150 eV by assigning to it the energy dependence of the closest relative, within the same series, that had been measured in the high-energy range. Such energy-extrapolated cross sections are enclosed in parentheses in Table I and are drawn with dashed lines in Fig. 4. Our measurements of the nP-$4S$ cross sections were made primarily at the single impact energy of 15 eV. Each of these excitation functions can safely be assumed to have the same energy dependence as the corresponding nP-$3S$ function, with which it shares a common upper level. This permits us to deduce the absolute $Q_{nP-4S}(E)$ at any energy E in terms of the directly measured values of $Q_{nP-4S}(15\ eV)$, $Q_{nP-3S}(15\ eV)$, and $Q_{nP-3S}(E)$. Values of $Q_{nP-4S}(E)$ included in Table I have been obtained this way.

Our nF-$3D$ measurements were also made at the single impact energy 15 eV, but for this series, unlike nP-$4S$, we have no experimental basis for deducing $Q_{nF-3D}(E)$ at other energies.

Several general observations can be made upon examination of Figs. 4 and 5. We see that the excitation functions of the three series shown have different characteristic features, and that within each family the excitation functions decrease in magnitude and evolve in shape in a regular, continuous manner as n is increased. In the sharp series the declining portion of the curve evolves into an S shape; the main peak becomes sharper and a relative minimum develops around 10 eV. A similar but less pronounced behavior occurs in the principal series. In the diffuse series the maximum gradually becomes flattened, and a distinct, angular shoulder develops just above threshold.

Within a given spectral series, and at a given impact energy, the dependence of the optical-excitation cross section $Q_{nL-n'L'}$ upon the effective principal quantum number n^*_{nL} of the upper level is given by

$$Q_{nL-n'L'} = C_L (n^*_{nL})^{-\alpha_L}, \tag{2}$$

where C_L and α_L are parameters associated with the different series. The main dependence on impact energy is carried by C_L, although α_L is not entirely energy independent. This formula applies to the upper members of each series; the cross section of the first member is 2–10 times larger, and of the second member 10–25% larger than predicted by Eq. (2). Excluding these the formula reproduces our experimental cross-section values for the remaining 17 members ($nL = 6S \cdots 9S$, $5P \cdots 8P$, $5D \cdots 9D$, $6F \cdots 8F$, and $12F$) of the S, P, D, and F series with an rms precision of 2.5%. For example, at a collision energy of 15 eV such a fit is obtained by the C_L values (in units of 10^{-18} cm^2)—$C_S = 6170$, $C_P = 28\,500$, $C_D = 22\,600$, and $C_F = 18\,600$, and α_L values—$\alpha_S = 4.61$, $\alpha_P = 6.02$, $\alpha_D = 4.44$, and $\alpha_F = 4.57$.

B. Summary of experimental uncertainties

Our estimates of the overall experimental uncertainties are given in the third column of Table I at a confidence level of 70%. These uncertainties are assigned to individual values of absolute excitation cross sections; the uncertainty in relative cross sections, i.e., the ratio of cross sections for a given line at two different impact energies, or the ratio of cross sections for two different lines at the same energy, is considerably smaller. The uncertainties break down as described in our potassium paper.[5] A representative uncertainty, 12%, might consist of several components added in quadrature, for example, 7% for number density, 7% for radiometric calibration, 5% for miscellaneous systematic errors, and 5% for miscellaneous random or statistical errors. The uncertainties vary from one transi-

tion to the next; we list below several errors which apply particularly to certain transitions.

Some of the infrared lines have greater uncertainty, 20–25%, on account of the poorer detection efficiency and the greater background light from the electron-gun filament. The farther ultraviolet lines have similarly large uncertainties originating in the radiometric calibration and the deteriorated uv transmittance of the collision chamber windows.

Errors associated with the anisotropy of emission have been eliminated or reduced as described in Sec. II, except for the fundamental series, for which an additional uncertainty of 10% is allowed.

The $3P$-$3S$ cross section is subject to errors arising from the scattering of resonance radiation. As explained in our potassium paper, the effect of resonance-line scattering upon Q_{3P-3S} is reduced to a few percent through a combination of experimental design of the collision region and operation at low number densities.

For highly excited states optical-excitation-cross-section measurements are subject to two additional errors, which have not been included quantitatively in our uncertainty estimates, but about which some semiquantitative statements can be made. Both of these involve mechanisms of transition between excited states other than the spontaneous radiative emission considered exclusively in our definition of Q_{jk}.

The first of these is the quenching of excited sodium atoms by collisions with ground-state sodium atoms. The relevant cross sections for this process have not been measured, but from recent experiments on related atomic systems it can be inferred that quenching to energetically nearby states is strongly favored, and that for such a transition the quenching cross section is likely to be of the same order of magnitude as the geometrical cross section of the excited state, which in the Coulomb approximation is given approximately by $\frac{5}{2}(n^*)^4\pi a_0^2$, a_0 being the first Bohr radius and n^* the effective principal quantum number.[21-23] By contrast, radiative decay rates decrease roughly as $(n^*)^{-3}$, so that the importance of quenching relative to radiative transitions increases rapidly with n^*.[24,25] The quenching reactions most likely to affect our results are those that change the orbital angular momentum—specifically, those that mix the nD states with the manifold of nearly degenerate $nF, G, H\ldots$ states lying only a few cm^{-1} higher. Making use of the above estimate for the quenching cross section, and assuming a density of 3×10^{12} atoms/cm^3 and an average interatomic speed of 10^5 cm/sec for Na at 275 °C, we find that for $n\gtrsim11$ the quenching rate of nD and nF states may compete with the radiative decay rate. Thus our cross-section results for the highest members of the diffuse and fundamental series should be regarded with some reservation. The fact that cross sections for these higher members do not deviate from the n^* power law [see Eq. (2)] established for lower members of the series gives at least some indication, however, that atoms in these higher states relax in the same way as those in lower states, i.e., via radiative decay.

The second mechanism of transition between excited states that we have not considered is the absorption of, and the stimulation of emission by, the cavity radiation present in the heated collision chamber. The effect of a room-temperature blackbody field upon the radiative lifetime of highly excited ($n=17,18$) P states of Na has been found by Gallagher and Cooke[26] to be quite pronounced. At the higher temperature of our experiment, 275 °C, these effects can be expected to extend to somewhat lower-lying levels. The radiant energy density peaks broadly at about 10^5 Å; at the much shorter wavelengths of the lines observed in our experiment, the field is negligibly weak and plays no direct role. Nevertheless, by inducing transitions among the closely spaced higher-lying levels, via absorption and stimulated emission, the blackbody field can alter the populations of the upper levels of the observed lines, thereby altering the intensities of these lines. An elementary analysis shows that the presence of a field of temperature T modifies the rate at which transitions occur from a level i to a lower level j according to

$$A_{ij}\rightarrow A_{ij}\left\{1+\left(1-\frac{N_j/g_j}{N_i/g_i}\right)\left[\exp\left(\frac{h\nu_{ij}}{kT}\right)-1\right]^{-1}\right\}, \qquad (3)$$

where A_{ij} is the spontaneous radiative-transition probability, ν_{ij} is the frequency, N_i and N_j are the populations, and g_i and g_j the degeneracies. Clearly this effect can either increase or decrease the effective transition probability, and can drive it negative, corresponding to net absorption from j to i. The effect is greatest when the levels involved are closely spaced and have very different N/g ratios. As a particular example, the upper P states, owing to their long lifetimes, are probably more heavily populated than the neighboring S and D states, and the blackbody field should act to restore statistical population ratios among these states. By absorption and stimulated emission the S (and to a lesser extent D) states should be populated at the expense of the P states, thereby enhancing the emission of the upper sharp series (and to a negligible

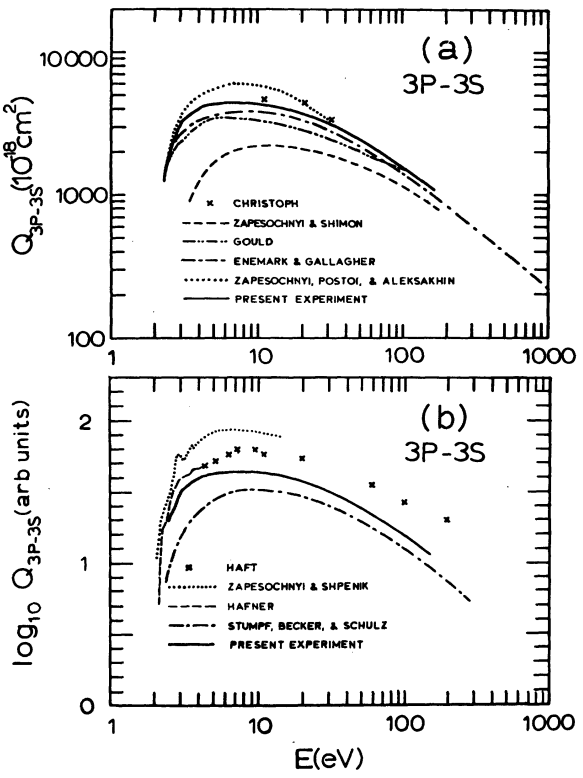

FIG. 6. Comparison of experimental results for the $3P$-$3S$ optical-excitation function. (a) Absolute and Born-normalized results, (b) relative measurements displaced vertically by arbitrary amounts for clarity of presentation.

extent the diffuse series) while weakening the principal series. Our cross-section results are not corrected for this effect, and thus, strictly speaking, should be identified with a temperature of 275 °C. Approximate calculations indicate that the effect on the cross sections can be neglected for the diffuse and fundamental series, but may amount to about 15% for uppermost members of the sharp and principal series.

C. Comparison with other experimental work

The optical excitation of the $3P$-$3S$ transition has been investigated experimentally by a number of workers over the years, with the results summarized in Fig. 6. Absolute and Born-normalized results are included in Fig. 6(a). The results plotted in Fig. 6(b) are relative only, i.e., they give only the shape of Q_{3P-3S}; these have been shifted vertically with respect to one another by arbitrary amounts for clarity of the display.

The earliest work, by Haft,[27] shows the general shape of Q_{3P-3S} but is now only of historical significance. This was followed by Christoph's[28] more refined, absolute measurements which were made at much lower densities and beam currents and incorporated an experimental correction for the effects of resonance-line scattering. Because there are only three points which are subject to substantial statistical fluctuation relative to one another, it is not meaningful to assign a "shape" to Christoph's results. His data can be compared with ours, point by point, however, and this produces agreement within 5–25%.

Zapesochnyi and his collaborators have obtained several results for Q_{3P-3S}. In a single-beam, static-gas-type experiment, in which the number density was determined by use of vapor pressure tables, Zapesochnyi and Shimon[29] measured the absolute cross section with a stated precision of 35% in the energy range from threshold to 150 eV with an energy resolution of 0.8 eV. In comparison with our curve, theirs falls off more slowly with energy, this difference diminishing at higher energies. At lower energies their excitation function lies below ours by a wide margin, typically by a factor of 2. The center of the broad maximum is located several volts above ours, and the initial ascent to the peak from threshold is comparatively slow and unmarked by structural detail. Subsequently, using a cylindrical electron monochromator to improve the energy resolution (0.25 eV), Zapesochnyi and Shpenik[30] reexamined the shape of the lower-energy (0–15 eV) portion of Q_{3P-3S} with markedly different results. The peak was narrowed and shifted towards lower energy by several volts, and some detailed structure was revealed on the ascending portion of the curve. In some respects this result agrees better with ours than does the previous one, and the resolved features at 2.8 and 3.5 eV could be higher-resolution manifestations of what appears in our Q_{3P-3S} as simply an abrupt change in slope at about 3 eV.

More recently, Zapesochnyi, Postoi, and Aleksakhin[4] have reported another absolute measurement of Q_{3P-3S}, made with crossed electron and atom beams, which contrasts sharply with both of the previous experiments of Zapesochnyi *et al.* The peak cross section is almost three times larger than the value of Zapesochnyi and Shimon, while the rate of descent at the high-energy limit of their published Q_{3P-3S} data, 30 eV, is a great deal steeper. In explanation of the discrepancies between this work and its predecessors, Zapesochnyi, Postoi, and Aleksakhin cite several deficiencies in the earlier work, including inaccurate number density determination and shape distortion by secondary electrons. With regard to both shape and magnitude, our curve is intermediate between the earlier and later results of

Zapesochnyi *et al.* and yet is not in agreement with either over a broad range of energies. At its peak, Zapesochnyi, Postoi, and Aleksakhin's Q_{3P-3S} is 32% higher than ours, which is difficult to explain in view of the uncertainties claimed—8% by Zapesochnyi *et al.* and 12% by us.

Better agreement is found with the results of four crossed-beam experiments done over the past decade, two of them Born normalized[3,31] and two of them relative.[32,33] From the 15-eV to the 150-eV limit of our experiment, our curve shape is in excellent agreement with those of Enemark and Gallagher[3] and of Stumpf, Becker, and Schulz.[33] The close mutual agreement of these three shapes and their convergence to the Born-approximation shape[34] at high energies seems to firmly establish the behavior of Q_{3P-3S} in this range. The slowness with which Gould's[31] curve falls off above about 60 eV is probably erroneous, as it does not approach the Born-theoretical curve smoothly (to be discussed in a later section), but rather crosses it at an oblique angle. Thus, although Gould has set his cross section (corrected for estimated cascade) equal to the Born value at the high-energy limit of his experiment, 100 eV, this does not constitute a true high-energy Born normalization, such as that of Enemark and Gallagher. While the normalization of Gould's Q_{3P-3S} and its shape at higher energies are open to question, this has no effect upon the relative shape at lower energies. A comparison of shapes of his excitation function with ours shows excellent agreement from about 30 eV down to below 3 eV. The low-energy range from threshold to about 4 eV was investigated in great detail by Gould and later by Hafner.[32] Our shape results are consistent with theirs, but in view of the superior energy resolution (0.07 eV for Gould, 0.05 eV for Hafner) and smaller beam currents used in their experiments, their shapes show the structure in finer detail and should be assigned greater weight than ours. The shape of Enemark and Gallagher's Q_{3P-3S} below 10 eV agrees with ours to a somewhat lesser extent. From threshold it rises somewhat more slowly to its peak with no irregular features along the way. The difference between their absolute Q_{3P-3S} and ours is at its largest, 17%, at about 4 eV. Of this amount about half can be considered a disagreement in normalization; this is the extent to which our curve is above theirs in the high-energy region where the two curves are parallel and where the Born normalization is applied. The remaining half represents the maximum extent of distortion of one curve relative to the other.

The shape difference between our Q_{3P-3S} and that of Stumpf, Becker, and Schulz[33] at low energy is more problematic. [Stumpf, Becker, and Schulz gave results for the separate components of the $3P$-$3S$ doublet. The single curve in Fig. 6(b) is the sum of these two components. Certain details of structure in their original data have not been reproduced in our graph.] Normalizing their relative excitation function to ours at high energy, we find that below 15 eV the two curves diverge, so that by about 3 eV their curve lies about 40% lower than ours, or alternatively, shifted locally towards higher energies by about 1.5 eV. This exceeds the limits we have anticipated for our experimental uncertainties.

Excitation of the nonresonance transitions has been less extensively investigated than that of $3P$-$3S$. No measurements have previously been reported for the leading member of the sharp series, the higher members of the principal series, nor for any of the fundamental series or the nP-$4S$ series, and the first member of the diffuse series has been measured only once. The most frequently studied cross sections, Q_{6S-3P} and Q_{5D-3P}, are shown in Fig. 7.

Haft's[27] early work is today of historical in-

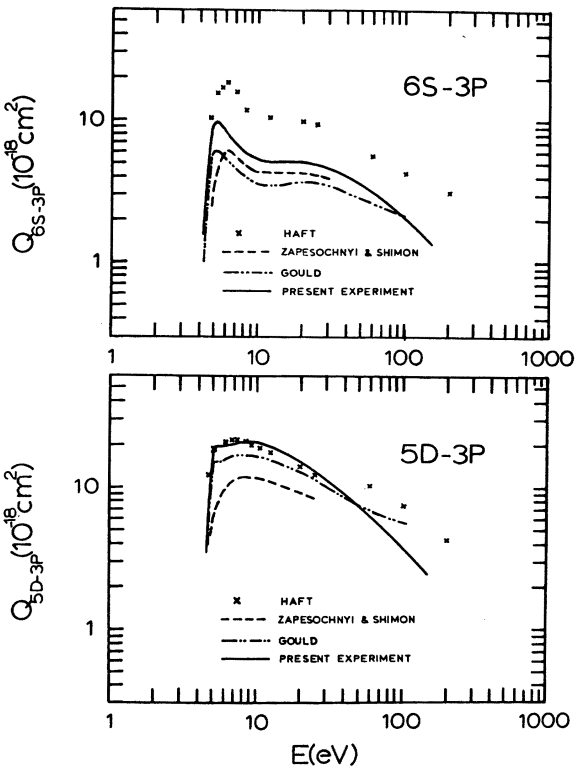

FIG. 7. Comparison of experimental results for $6S$-$3P$ and $5D$-$3P$ optical-excitation functions.

terest only. His calibration was evidently invalid, so that only the shapes of the excitation functions retain significance. The three higher-energy data points of Q_{5D-3P} seem to be discontinuous with the lower-energy data.

Volkova[17] measured absolute cross sections, at the peak only, for a number of diffuse series transitions ($n=4,6,7,8,9$) using photographic detection and standardizing against previously measured helium cross sections. In view of the current obsolescence of these methods, as well as the very large (200-μA) beam currents employed and the serious problems experienced with window darkening, Volkova's values, typically 2–5 times smaller than ours, should be assigned considerable uncertainty.

Zapesochnyi and Shimon[29] reported absolute peak cross sections for 18 sharp, principal, and diffuse transitions and gave the energy dependence to 30 eV for the many of these. This has been the largest body of experimental cross sections to date. For a few lines, i.e., $3D$-$3P$, $5S$-$3P$, and $6S$-$3P$, our absolute cross sections agree with theirs within 20%, at least over a restricted range near 10 eV. For the uv line $5P$-$3S$, however, their value is about 40 times smaller than ours, suggesting severe problems with scattered light (see Sec. II A) or deterioration of the uv transmittance of their excitation tube. The remaining cross sections are typically about half as large as ours and differ markedly in shape, as we have seen with Q_{3P-3S}. In general, they do not rise as steeply to the peak following threshold as do ours. For the sharp series their peaks are located at about 1-eV higher energies than ours and do not rise as high above the plateau region located between 10 and 20 eV. For the upper diffuse series their results do not show the angular shoulder just above threshold, although for the first two members of this series such a structure can be discerned in its incipient form in their curves, as in ours.

Gould[31] has determined the excitation functions of two nonresonance transitions, $6S$-$3P$ and $5D$-$3P$. In general shape as well as structural detail his curves are in good agreement with ours below about 30 eV. This agreement is noteworthy in view of the considerable differences in collision geometry and other particulars of the two experiments. With increasing energy, however, the shapes of Gould's curves differ markedly from ours, and they diverge from the E^{-1} high-energy dependence predicted by the Born approximation.[35] As we have already discussed in connection with Q_{3P-3S}, this divergence from Born theory would seem to limit the validity of Gould's normalization procedure, which was only approximate in any case, since no allowance was made for cascade population of $6S$ and $5D$.

IV. DIRECT-EXCITATION FUNCTIONS

From our experimentally measured cross sections for the production of spectral lines, $Q_{jk}(E)$, we can determine the cross section for direct excitation of the various levels by electron impact. As explained in our potassium paper,[5] the direct-excitation function $Q_j(E)$ for a level j can be expressed as a linear combination of the optical-excitation functions of the relevant transitions, specifically, one transition originating in j and one in each state i that decays radiatively to j. The transformation is given by

$$Q_j(E)=\frac{1}{A_{jk}\tau_j}Q_{jk}(E)-\sum_{i>j}\frac{A_{ij}}{A_{im}}Q_{im}(E). \qquad (4)$$

Here $j\rightarrow k$ is the experimentally observed transition originating in j, A_{jk} is the corresponding spontaneous radiative transition probability, and τ_j is the radiative lifetime of j. Thus, the first term on the right-hand side, which we will refer to as the apparent cross section of j, gives the total of all optical-excitation functions originating in j in terms of an experimental measurement of any one of them, Q_{jk}.

The second term on the right-hand side of Eq. (4) gives the total cross section for population of j by radiative cascade from higher levels i. Here $i\rightarrow j$ is a cascade transition, which in many cases lies too far in the infrared to be experimentally accessible, while $i\rightarrow m$ denotes some other experimentally observable transition originating in the same level i. Thus the term $(A_{ij}/A_{im})Q_m$ gives the $i\rightarrow j$ cascade in terms of the measurable cross section Q_{im}.

The Q_j's determined by Eq. (4) will be referred to as our experimental direct cross sections since they are derived from experimentally measured Q_{jk}'s. However, they also depend in varying degrees upon the values adopted for the transition probabilities, all of which have been taken from compilations in the literature, and many of which are theoretical in origin. Because of this dependence we discuss our selection of A_{jk} values in detail.

A. Selection of transition probabilities

With several important exceptions to be enumerated below, we used the transition-probability values calculated by Lindgard and Nielson,[26] using Coulomb-approximation wave functions. These are in very good agreement with the calculations of Anderson and Zilitis[37] and of Biemont and Grevesse,[38] and with almost all of the experi-

mental lifetime measurements of Gallagher, Edelstein, and Hill[24,25] and of Kaiser.[39] We now discuss the exceptions, i.e., the cases where we did not adopt Lindgard and Nielsen's values. Selection of values for A_{3P-3S}, A_{4S-3P}, and A_{3D-3P} was unnecessary since these do not enter the transformation equations at all, there being no branching from the upper levels, $3P$, $4S$, and $3D$. Values for A_{4D-3P}, A_{4D-4P}, and A_{8P-3S} were taken from the critical compilation of Wiese, Smith, and Miles,[18] and are based upon a combination of theory and experiment. These values do not differ from those of Lindgard and Nielson by more than 8% so the substitution has little effect on the Q_j's.

For A_{nP-3S} and A_{nP-4S} ($n=4, 5, 6, 7$) we had to modify the values given by the sources cited above so as to make them consistent with our own experimental observations. The necessity for this modification arose as follows. For each of the three levels $5P$, $6P$, and $7P$, we have measured optical-excitation cross sections for two decay modes, rather than just one, namely, for transitions terminating in $3S$ and in $4S$, as shown in Table I and Fig. 1. From our measurements of Q_{nP-4S} and Q_{nP-3S} we compute the three ratios Q_{nP-4S}/Q_{nP-3S} for $n=5$, 6, and 7. Each of these experimental Q_{jk} ratios should agree with the corresponding ratio of transition probabilities, A_{nP-4S}/A_{nP-3S}, using A_{jk} values from the literature sources already cited. When the comparison is made, however, some disagreement is found. Our cross-section ratios are 1.54, 1.29, and 1.31 for $n=5$, 6, and 7, while the respective transition-probability ratios of Wiese *et al.*[18] are 1.23, 1.02, and 0.87. The equations transforming optical to direct cross sections are based upon the assumption of equality of these A_{jk} and Q_{jk} ratios, and ambiguities result if these ratios are independently specified. To remove these ambiguities either the A_{jk} or Q_{jk} ratios must be changed. We believe the A_{jk} ratios are more likely to be in error, particularly for the principal series, which are based upon theoretical calculations of 50 years ago. Despite the 25% uncertainty assigned to these particular values,[18] a larger error may be possible as indicated by recent remeasurements of the oscillator strengths of the principal series of potassium.[40] Our experimental Q_{jk} ratios are likely to be more reliable because some of the principal systematic errors, such as those in the number density, cancel out in this ratio. Thus we choose to modify the A_{jk} ratios to bring them into agreement with our measured Q_{jk} ratios for these transitions. To reduce the ratio A_{nP-4S}/A_{nP-3S} one might either decrease the numerator alone or else increase the denominator alone. The difference in the final direct-excitation functions resulting from these two alternative ranges from 10 to 25%. We choose instead a compromise method that results in A_{jk}'s and Q_{jk}'s that are intermediate between these extremes. For $n=5, 6, 7$ we change both the numerator and the denominator, i.e., A_{nP-4S} and A_{nP-3S}, in such a way that their ratio becomes equal to our measured Q_{nP-4S}/Q_{nP-3S}, while their sum remains unchanged. In this way none of the A_{jk}'s needs to be changed by as much as 25%, while the lifetimes deduced from the A_{jk}'s remain unchanged. This is desirable since the lifetimes are in good agreement with experimental values[25] (3% for $5P$ and $6P$; the discrepancy is larger for $7P$, 17%, but this is not so critical since we do not attempt to determine the direct cross section for this state). The values adopted, in units of MHz, are $A_{5P-3S}=0.528$, $A_{5P-4S}=0.813$, $A_{6P-3S}=0.199$, $A_{6P-4S}=0.258$, $A_{7P-3S}=0.096$, and $A_{7P-4S}=0.127$.

The final instance in which we modified the value of an A_{jk} from the literature is that of A_{4P-3S}. There are two reasons for this alteration. First, it seems likely that the trend observed for 5, 6, and $7P$, in which the ratio of published transition probabilities A_{nP-4S}/A_{nP-3S} is evidently too small, may extend to the next lowest member $4P$. Secondly, the $4P$ lifetime computed by summing values of A_{4P-4S}, A_{4P-3S}, and A_{4P-3D} given by Wiese *et al.* is 0.107 μs, which is considerably smaller than the directly measured value, $\tau_{4P}=0.125\pm0.010$ μs, due to Gallagher, Edelstein, and Hill.[25] The extent of this discrepancy is greater than for any of the 20 other S, P, and D states (except $7P$) measured by Gallagher, Edelstein, and Hill,[24,25] and/or by Kaiser.[39] These circumstances suggest that if the A_{4P-4S} and A_{4P-3S} values of Wiese *et al.* are used, then the computed ratio A_{4P-4S}/A_{4P-3S} will be too small and the sum $A_{4P-4S}+A_{4P-3S}$ too large (the third member of this sum A_{4P-3D} is very small and can be neglected as a source of error in calculating τ_{4P}). To remedy this we have made a moderate decrease in A_{4P-3S} (from 2.92 to 2.56 MHz) while holding A_{4P-4S} at its published value of 6.20 MHz. There is a degree of arbitrariness in the particular choice of values, but this approach alleviates the difficulties cited above while avoiding extremes in the values of A_{4P-4S} and A_{4P-3S} and in the direct cross sections Q_{4P} and Q_{4S} that are dependent on them.

The transition probability values cited by Wiese *et al.* are assigned a 25% or better uncertainty. The confidence level is not explicitly stated but is evidently fairly high—we assume about 95%. The other sources do not give uncertainty estimates, but since their results are in fair agree-

TABLE II. Experimental optical-, apparent-, cascade-, and direct-excitation cross sections of sodium.

Level j	Cross section (10^{-18} cm^2) at energy 15 eV: Observed optical ($j \rightarrow k$)	Apparent	Cascade	Direct
$4S$	187.0 ($4S$-$3P$)	187.4	100	87.4
$5S$	20.1 ($5S$-$3P$)	35.1	17.4	17.7
$6S$	5.14 ($6S$-$3P$)	10.41	3.84	6.57
$7S$	2.05 ($7S$-$3P$)	4.42	1.04	3.38
$3P$	4050 ($3P$-$3S$)	4050	660	3390
$4P$	36.6 ($4P$-$3S$)	125.4	65.4	60.1
$5P$	5.62 ($5P$-$3S$), 8.66 ($5P$-$4S$)	30.1	14.7	15.4
$6P$	1.47 ($6P$-$3S$), 1.90 ($6P$-$4S$)	8.58	4.47	4.11
$3D$	354 ($3D$-$3P$)	354	65[a]	289
$4D$	54.1 ($4D$-$3P$)	81.8	13.7[a]	68.1
$5D$	17.8 ($5D$-$3P$)	33.5	3.9[a]	29.6
$6D$	7.91 ($6D$-$3P$)	16.3	1.3	15.0
$6F$	5.03 ($6F$-$3D$)	9.71	0.16[b]	9.55
$7F$	2.47 ($7F$-$3D$)	5.35	0.09[b]	5.26

[a] These cascade figures are inclusive of estimated amounts of cascade from $4F$ and $5F$. We estimate that $3D$ receives 40 units of cascade from $4F$ and 12 units from $5F$, that $4D$ receives negligible cascade from $4F$ and 6.6 units from $5F$, and that $5D$ receives negligible cascade from $5F$. The quoted direct D-state cross sections are corrected for this estimated cascade.

[b] These cascade figures are exclusive of cascade from G levels. Thus the cited F-state direct cross sections include an unknown amount of cascade from G states. We estimate this cascade to be quite small, as explained in text.

ment with those of Wiese *et al.*, we assume that a similar degree of uncertainty applies to them.

B. Results for direct-excitation functions

With the above choice of transition probabilities, along with our measured optical-excitation functions, we have determined the direct-excitation functions for 12 excited states, namely, for the 4 lowest members of the S, P, and D families. We have also determined the direct cross sections of the $6F$ and $7F$ states at a single energy 15 eV. Table II gives a breakdown of the excitation of sodium at 15-eV impact energy. For each excited state we identify the decay transition observed and its optical-excitation cross section, the direct cross section, the cross section for excitation of the level by cascade, and the apparent cross section which is the cross section for excitation of the state by the combined direct and cascade processes.

The direct-excitation cross sections at selected energies are tabulated in Table III. The uncertainties listed incorporate experimental errors in the optical-excitation cross sections as well as estimated uncertainties in the transition probabilities. Other errors associated with the truncation of the cascade series, collisional quenching, absorption of and emission stimulated by the blackbody field, etc., are estimated to be much smaller than these for the states of interest ($n \leq 7$). The cited uncertainties correspond to a 70% confidence level.

The direct-excitation functions for S, P, and D states are graphed logarithmically in Fig. 8, along with the Born-approximation calculations of Vainshtein,[34] which will be discussed in Sec. IV D. A comparison of this figure with Fig. 4 shows how cascade and branching corrections alter the shape and magnitude of the optical-excitation functions to yield the direct-excitation functions. It is interesting to note that for the S family the removal of cascade reveals direct-excitation functions that have sharper, narrower peaks and bear a closer resemblance to one another than do members of the "parent" family of optical-excitation functions, i.e., the sharp series. The same comments apply, but to a lesser extent, to the D family. In the P family cascade subtraction reveals a shallow relative minimum in Q_{3P} at about 5.3 eV, as well as a number of irregular features in the higher

TABLE III. Experimental direct-excitation functions of sodium.

Level j	Uncertainty[a] (%)	Direct-excitation cross section $Q_j(10^{-18}$ cm$^2)$ at E (eV) 5	7	10	15	20	30	50	75[b]	100[b]	150[b]
$4S$	40	141	112	97.1	87.4	82.1	72.4	57.2	45.3	39.5	(26.1)
$5S$	40	36.1	22.6	19.4	17.7	17.4	14.7	11.8	8.81	7.15	4.55
$6S$	30	15.6	9.34	6.76	6.57	6.42	5.77	4.69	3.70	2.65	1.76
$7S$	25	4.97	4.71	3.67	3.38	3.45	3.07	2.57	1.84	1.36	0.93
$3P$	12	3490	3600	3560	3390	3180	2750	2230	1730	1390	1020
$4P$	40	79.2	60.5	58.5	60.1	57.8	50.5	39.3	27.9	22.1	15.6
$5P$	40	17.5	16.9	14.3	15.4	14.8	14.1	10.4	7.82	6.41	4.81
$6P$	40	5.13	5.40	4.12	4.11	4.49	4.39	3.25	(2.48)	(2.01)	(1.53)
$3D$[c]	15	397	412	367	289	235	167	106	67.8	50.9	32.7
$4D$[c]	20	49.3	87.0	84.2	68.1	55.0	40.7	26.3	18.1	13.7	8.95
$5D$[c]	20	26.7	34.4	34.6	29.6	24.8	18.6	12.3	8.44	5.98	4.04
$6D$	20	8.48	16.2	16.8	15.0	13.1	9.59	6.44	4.20	3.12	1.94
$6F$[d]	25				9.55						
$7F$[d]	25				5.26						
Total inelastic[e]	10	4340	4500	4380	4090	3780	3220	2560	1960	1570	1140

[a] Uncertainties correspond to 70% confidence level.
[b] Values in parentheses are based upon extrapolations in energy.
[c] The $3D$, $4D$, and $5D$ cross sections are based upon estimated amounts of cascade from $4F$ and $5F$, as explained in text.
[d] The F cross sections have not been corrected for the unknown cascade from the G levels.
[e] Obtained by summing the optical-excitation cross sections of the principal series.

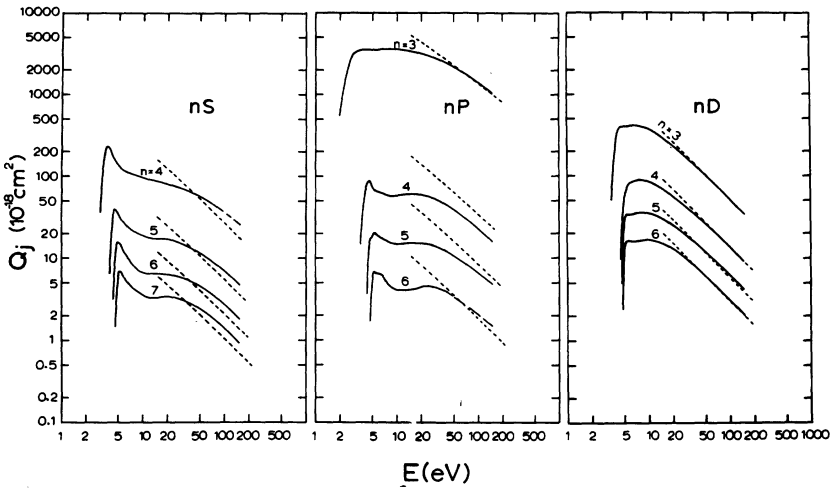

FIG. 8. Direct-excitation functions for S, P, and D states of sodium. Solid curves are present experimental results and the long-dashed portion of the $4S$ and $6P$ curves are extrapolations. The short-dashed curves are the Born-approximation calculations of Vainshtein *et al.*

members below 10 eV. Similar observations have been made for potassium, and a comparison of Fig. 8 of the present paper with Fig. 9 of Ref. (5) clearly shows the kinship of these two elements.

We now discuss the direct-excitation functions of the various states individually, emphasizing the branching and cascade analysis and the final precision.

1. 3P state

This state has the largest and most accurately determined direct cross section. The comparatively high precision is due to the fact that the entire emission from this level occurs in a single, directly measured doublet, while the various cascade transitions, which contribute less than 20% of the total rate of $3P$ excitation, are also directly measured. Hence, there is no dependence upon transition probabilities.

2. 4S state

Throughout much of the energy range, cascade is of equal or greater importance than direct excitation as the process responsible for populating $4S$. When this cascade, 85% of which comes from $4P$, is subtracted from the $4S$-$3P$ optical-excitation function, a very narrow, sharply peaked Q_{4S} is revealed. Because of the narrowness of this peak, its exact height and detailed structure are particularly susceptible to errors arising from the finite-energy width of our beam and from any small differences between the energy scales of Q_{4P-3S} and Q_{4S-3P}, such as may arise from varying space charges or contact potentials. The sizable cascade from $4P$ has the effect of introducing into Q_{4S} a strong dependence upon the transition probabilities A_{4P-4S} and A_{4P-3S}. This subjects Q_{4S} to additional uncertainties which exceed the experimental errors arising from the rather unfavorable wavelengths (11 382–11 404 Å) of the observed transition $4S$-$3P$. Fortunately, there is no radiative branching from $4S$ so there are no unobserved radiative transitions to further degrade the precision of Q_{4S}, which we place at 40%.

3. 5S state

The analysis of this level is similar to that of $4S$, except that the dominant cascade into $5S$ comes from $5P$. The observed emission lines from $5S$, i.e., $5S$-$3P$ doublet, are in a more easily accessible part of the spectrum than in the preceding case, but this is offset by the fact that this transition does not represent the entire emission from $5P$, 40% of which occurs by the unobserved $5S$-$4P$ transition. The final uncertainty is 40%.

4. 6S and 7S states

The precision of these levels, 30% and 25%, is improved relative to that of $4S$ and $5S$, reflecting the reduced importance of cascade.

5. 4P state

For the $4P$ state, unlike $3P$, cascade is of approximately the same importance as direct excitation. It is contributed in comparable amounts by S and D levels, and has a strong effect on the shape of the Q_{4P} curve, particularly near the

peak. The decay from this level is divided between $4P$-$4S$ and $4P$-$3S$, with the unobserved $4P$-$4S$ transition being the stronger. The result is a rather low precision, 40%.

6. 5P and 6P states

These are similar to $4P$ but have even more branching. Moreover, the observed lines are weaker and lie farther in the uv, increasing the experimental uncertainties. The irregular structures near the peaks may simply be artifacts of the cascade analysis. The portion of Q_{6P} above 50 eV is based upon extrapolation. Thus, the precision is poor, 40%.

7. 3D state

The principal uncertainties here occur in the cascade correction. The cascade from P levels is almost negligible on account of the smallness of the relevant transition probabilities A_{nP-3D}. Thus the cascade into $3D$ is confined to the fundamental series transitions nF-$3D$. We had to make estimates of this cascade since, as discussed earlier, our measurements of the nF-$3D$ series covered only $n=6$, 7, 8, and 12, and even in these cases only for a single impact energy, 15 eV. To estimate the unobserved cascade from the F's we made use of the trends observed in the other spectral series as well as the empirical relationship Eq. (2). The resulting estimated values of Q_{nF-3D} (15 eV) are 40.0×10^{-18}, 12.0×10^{-18}, 0.8×10^{-18}, 0.5×10^{-18}, and 0.3×10^{-18} cm^2 for $n=4$, 5, 9, 10, and 11, respectively. Then, to approximate the energy dependence of this cascade, we assumed that each $Q_{nF-3D}(E)$ had the same shape as the $Q_{nD-3P}(E)$ with the same n, these latter excitation functions having been experimentally observed at all energies. This assumption is suggested by our studies of potassium, which found the diffuse and fundamental series optical-excitation functions to have similar shapes. While the approximation is rather crude, we do not anticipate that a large error in Q_{3D} will result, since the total cascade accounts for less than 20% of the total rate of population of $3D$. Some distortion of shape could result, and this would be most noticeable in the peak region. The resultant precision 15% is second only to that of Q_{3P}.

8. 4D, 5D, and 6D states

These levels resemble $3D$ except that they have radiative branching, which increases for the higher nD levels. In each case, however, at least 50% of the total radiative decay occurs via the observed multiplet, so the problem is less serious here than for the P levels. Moreover, the importance of the cascade decreases with higher n; by $n=6$ cascade provides less than 10% of the excitation. Thus, the overall uncertainties are moderately low, 20%.

9. 6F and 7F states

The observed $6F$-$3D$ and $7F$-$3D$ multiplets carry about 50% of the decay of these levels. The cascade from the D levels is very small. The cascade from the G's is not accessible to our experiment, so we have not corrected the Q_{nF}'s for it. We have carried out Born calculations for the Q_{nG}'s, which indicate that G levels produce little cascade into the F's. If this is the case then the Q_{nF} values given in Tables II and III, uncorrected for G cascade, should be valid.

We do not have sufficient information to determine the energy dependence of the Q_{nF}'s, so values are cited only for 15 eV.

10. Total inelastic cross section

As explained in our potassium paper, the total inelastic cross section Q_{TI}, defined as the sum of the direct cross sections of all excited states, is equal to the sum of the optical-excitation cross sections of the principal series,

$$Q_{TI} \equiv \sum_j Q_j = \sum_{n\geq 3} Q_{nP-3S} . \tag{5}$$

As can be seen from Table I, the leading term Q_{nP-3S} dominates to such an extent that we can approximate Q_{TI} by Q_{3P-3S} alone within about 1%. The overall uncertainty is 10%.

C. Comparison with other experiments

Zapesochnyi[41] has reported peak values for a number of S, P, and D direct cross sections and has given the energy dependence of Q_{3P} from 0–30 eV. His values are considerably lower than ours; for example, for Q_{3P} he cites a peak value of 2300×10^{-18} cm^2 vs 3600×10^{-18} cm^2 for our experiment. It is not clear how Zapesochnyi's value was obtained since the experimental optical-excitation cross sections upon which it is based are not given in his paper or its references. Moreover, his value is inconsistent with the optical-excitation data published previously by Zapesochnyi and Shimon,[29] which would yield a peak Q_{3P} of approximately 1600×10^{-18} cm^2.

Gould,[31] Enemark and Gallagher,[3] and Zapesochnyi, Postoi, and Aleksakhin[4] have all determined the direct-excitation function Q_{3P} based upon measurements of Q_{3P-3S}. We have already discussed their Q_{3P-3S} results and compared them with ours in Sec. III C. The remarks made there apply to Q_{3P} as well, since it differs from Q_{3P-3S} by only 20% or less the amount of

the cascade. The cascade corrections made by Gould, by Enemark and Gallagher, and evidently those by Zapesochnyi, Postoi, and Aleksakhin are all based upon the earlier optical-excitation date of Zapesochnyi and Shimon. Thus these results are not entirely independent, particularly at the lower energies, where the effect of cascade is maximum.

In contrast to the experiments cited thus far, which have all used optical detection of the excited atoms to study the excitation process, several recent experiments have measured the energy-loss spectrum of the inelastically scattered electrons instead. This allows determination of the angular dependence of the scattering and permits study of the direct-excitation process without the complications of radiative cascade.

Buckman and Teubner[42] determined the angular dependence of the scattering into the $3P$ channel between 2° and 145° at energies of 54.4, 100, 150, and 217 eV. At each energy this curve was normalized to the Born-approximation calculation of the differential cross section in the near-forward direction, and then integrated over all angles to yield the direct cross section Q_{3P}. The results, in units of 10^{-18} cm^2, are 2190 at 54.4 eV, 1340 at 100 eV, and 940 at 150 eV in good agreement with our values 2100, 1390, and 1020, respectively. Of course the nature of the normalization is such that this comparison is not very different from a direct comparison of our results with the angle-integrated Born cross section, to be taken up in the following section.

In the same type of experiment Srivastava and Vuskovic[43] have determined the direct cross section for excitation of the $4S$ state, the unresolved $(3D+4P)$ states, and the unresolved $(4D+4F+5P+5S)$ states, measured relative to the direct cross section of the $3P$ state. At each impact energy (10, 20, 40, and 54.4 eV) and scattering angle (10° to 140°) the scattered-electron-energy-loss spectrum determines the relative magnitudes of the differential cross sections of the several excited states. Angle integration then yields the relative direct-excitation cross sections, and the adoption of a standard value for the absolute cross section of any one of the states establishes the absolute-cross-section scale for all the others. For this normalization standard Srivastava and Vuskovic chose the $3P$ direct cross section of Enemark and Gallagher,[3] which as we have already discussed is itself normalized to the Born approximation and makes use of the cascade measurements of Zapesochnyi and Shimon.[29] To avoid such compounding of normalizations and permit a more direct comparison of our results with those of Srivastava and Vuskovic, we have renormalized their results to our own value of Q_{3P}. This enables a meaningful comparison to be made for the states other than $3P$. When this is done it is found that on the average (over all four energies and all three single or combined non-resonance states of Srivastava and Vuskovic's experiment) their cross sections are only a few percent lower than ours, which is much less than the experimental uncertainties of either experiment. Point by point, however, there is a considerable degree of random fluctuation of Srivastava and Vuskovic's values relative to ours, the rms amount being 25%. This may be a reflection of the uncertainty involved in carrying out the angular integration, which involves an extrapolation from 10° back to 0°, through a region which accounts for the great bulk of the integrated cross section (95% for $3P$) since the scattering is strongly forward peaked.

D. Comparison with theory

In this section we compare our experimental cross sections with several of the many available theoretical calculations, most of which have been reviewed in Refs. 1 and 2. We will focus on theoretical works that treat the excitation not only of $3P$ but of the next several excited states as well. For this comparison we divide the impact-energy scale into three ranges, high (>50 eV), medium (5–50 eV), and low (<5 eV), corresponding in a rough way to the regions of applicability of the theoretical models and approximations considered.

1. High energy

At sufficiently high energies the Born approximation is considered valid. An extensive set of Born cross sections of sodium covering all S, P, and D states up to $n=7$ has been calculated by Vainshtein, Opykhtin, and Presnyakov.[34] Overall confirmation of their results can be found in subsequent calculations employing the Born, Bethe, and Ochkur approximations.[44–46]

In Fig. 8 the Born cross sections of Vainshtein *et al.* have been plotted along with our experimental direct cross sections. We see that in the high-energy range, theory and experiment are in good agreement for the $3P$ state and for the entire D family. The comparison is especially significant for these particular states, since as noted earlier they are the ones for which the uncertainties in our experimental direct cross sections are the least (12–20%). In the important case of $3P$ it appears that our absolute experimental cross section is several percent larger than it would be if it were normalized to Vainshtein's Born cross section at asymptotically high

energies. For the entire S family the Born cross sections at high energies are consistently 20–30% lower than the experimental values, while for the upper P family the discrepancy between theory and experiment varies in magnitude and sign among the different members. For all these S and upper P states the extent of the disagreement is consistent with the overall uncertainties we have estimated for our experimental results, 25–40%.

The nature of the comparison between experiment and Born theory for sodium S, P, and D states is very similar to that found for potassium, except that for potassium it was the S states for which theory and experiment were in good agreement, while for the D's the Born cross sections were 30–45% smaller than our experimental values.

For higher-angular-momentum states, Born cross sections have previously been unavailable in the literature (except for the $4F$ state[44,45]), so we have carried out such calculations for a number of these states, namely, $4F$, $5F$, $6F$, $5G$, $6G$, and $7G$. Our calculations used the Roothaan-Hartree-Fock wave functions of Clementi and Roetti[47] for the ground state and hydrogenic wave functions for the excited states. (The adequacy of the hydrogenic wave functions is suggested by the smallness of the quantum defect of these states, 0.0014 or less, which indicates that there is little core penetration by the excited electron.) In the high-energy limit these Born cross sections are given by $Q_j(E) = A_j/E$, where $A_{4F} = 192$, $A_{5F} = 116$, $A_{6F} = 70$, $A_{5G} = 4.1$, $A_{6G} = 3.8$, and $A_{7G} = 2.9$, all in units of 10^{-18} cm^2 eV. (Our A_{4F} value is about 25% higher than previously calculated values.[44,45]) It is interesting to note that the first few Q_{nG}'s decrease rather slowly with n, and that they are more than an order of magnitude smaller than the corresponding Q_{nF}'s. The small size of the Q_{nG}'s relative to the Q_{nF}'s suggests that F levels do not receive a great deal of radiative cascade from G levels, so that our neglect of this cascade in the determination of our experimental Q_{nF}'s (Tables II and III) probably does not lead to serious errors.

The comparison between experiment and Born theory for the F states is somewhat limited in scope because we have both theoretical and experimental values for only one state, $6F$, at one impact energy, 15 eV. At this energy our Born theoretical value of Q_{6F} is about 50% smaller than our experimental value; and since, generally speaking, experimental cross sections in this energy range tend to fall off less rapidly with energy than do the Born cross sections, we can infer that in the high-energy range the discrepancy between experiment and theory would be at least this large. The disagreement probably extends to other F states as well, as we have seen in the case of potassium,[5] where theoretical values of $Q_{nF}(n = 5, 6, 7)$ are 30–50% smaller than the experimental values. The discrepancy for sodium exceeds the 20–25% uncertainties we have assigned to our experimental Q_{nF}'s. The fact that our experimental Q_{nF}'s may be erroneously high on account of the F levels being populated by the collisional quenching of nearby D levels (see Sec. III B) does not seem likely but cannot be ruled out. A more probable explanation is that the calculated F cross sections are too small, not necessarily because of inapplicability of the Born approximation itself but because of the inaccuracy of the wave functions used in the calculation. The matter of wave-function inaccuracies will be discussed further in Sec. IV D 4. (See also Sec. V C 1 of Ref. 5.)

The total inelastic cross section Q_{TI} in the Born approximation may be obtained simply by adding together the Born cross sections for the individual states. At 150 eV the sum of all 20 of the aforementioned calculated cross sections (covering all states with $n \leq 7$, $l \leq 4$, except $7F$) is 1119 $\times 10^{-18}$ cm. To this we add an estimated truncation error of 6×10^{-18} cm^2 to cover all states with $n > 7$, $l > 4$, and $7F$ yielding a total inelastic Born cross section of 1125×10^{-18} cm^2 at 150 eV. This is in excellent agreement with our experimental value which is 1140×10^{-18} cm^2, with an error margin of 10% (see Table III).

The total inelastic cross section is so strongly dominated by the $3P$ channel that the above comparison between experiment and theory of Q_{TI} provides little information on the extent to which experiment and Born theory agree for the set of states other than $3P$, considered as a whole. As pointed out in our previous work (Sec. V C 1 of Ref. 5) there is an additional comparison between experiment and theory that can be made for this group of states based upon the equality

$$\sum{}' Q_j = \sum_{n \geq 4} Q_{nP-3S} + \sum_{n \geq 4} Q_{nS-3P} + \sum_{n \geq 3} Q_{nD-3P}, \tag{6}$$

where $\sum'$ is a summation over all j except $3P$. The left-hand side is evaluated by using the Born cross sections at 150 eV, yielding 110×10^{-18} cm^2, to which a truncation error of 6×10^{-18} cm^2 is added, for a total of 116×10^{-18} cm^2. This theoretical value is then compared with the experimental value, which is obtained by substituting into the right-hand side all of the experimental optical-excitation cross sections of the sharp,

principal, and diffuse series (except Q_{3P-3S}) at 150 eV as given in Table I. The resulting experimental value is 119×10^{-18} cm^2, and its precision is comparatively high since it does not depend on any radiative-transition probabilities. Comparing the above two values we see that experiment and Born theory give essentially the same result for the high-energy cross section for direct excitation of the group of states lying above $3P$.

2. *Intermediate energy*

In the intermediate energy range of 5–50 eV calculations of excitation cross sections for the $3P$, $3D$, $4S$, $4P$, $4D$, and $4F$ states by means of the method of multistate close coupling have been reported by Korff *et al.*[44] The wave functions of the electron-atom system were expanded by two states $(3S, nL)$, by three states $(3S, 3P, 3D)$, by seven states $(3S, 3P, 3D, 4S, 4P, 4D, 4F)$, and by eight states $(3S, 3P, 3D, 4S, 4P, 4D, 4F, 5P)$ of the target atom. Comparison of the cross sections derived from the different basis sets enabled them to monitor the convergence of the multistate-close-coupling expansion. Electron exchange between the colliding electron and target electron was neglected in their work. The impact energies considered were 7.36, 10.52, 16.83, and 23.14 eV.

The $3P$ cross sections calculated by Korff *et al.* are in good overall agreement with our experimental results, as shown in Fig. 9. The 0–15% difference in absolute values is not inconsistent with our experimental uncertainties, although there is some disagreement in shape at the lower energies. Among the six excited-state cross sections computed by Korff *et al.*, Q_{3P} can be considered the most reliable from the standpoint of convergence of the close-coupling expansion. Comparison of the three-state and seven-state calculations of Q_{3P} shows typical differences of only a few percent.

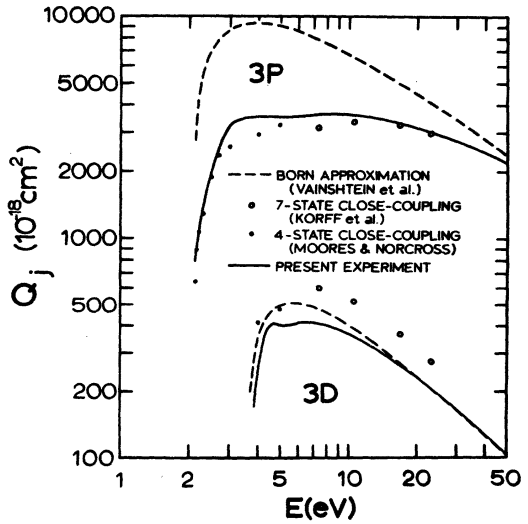

FIG. 9. Direct-excitation functions for $3P$ and $3D$ states: comparison of present experimental results with Born and close-coupling calculations.

Turning to the $3D$ state we find a more substantial discrepancy, the seven-state close-coupling calculations exceeding our experimental cross sections by 30–45%. Disagreement of this extent is outside the bounds of experimental error, so we consider possible sources of error in the theoretical calculation, including inaccuracies in the target-atom wave functions (Hartree-Fock-Slater-type), neglect of the atomic core interactions, incomplete convergence of the close-coupling expansion, and neglect of exchange between the incident electron and the atomic valence electron. Among these the neglect of core interactions has been justified by Korff *et al.* and the convergence of the close-coupling expansion, while less complete for $3D$ than for $3P$, seems to be adequate. A likely source of error then would be the neglect of exchange. Close-coupling calculations of $1s \rightarrow 2p$ excitation of H and the $X^1\Sigma_g^+ \rightarrow B^1\Sigma_u^+$ excitation of H_2 have demonstrated that the neglect of exchange can lead to a significant increase in the calculated cross sections, and that while the error introduced is greatest at low energies, it can persist to energies as high as several threshold units.[48,49]

From Fig. 9 it is evident that the Born calculation of Q_{3D} actually agrees better with our experimental result than does the close-coupling calculation. This is unexpected inasmuch as no claims are made for the Born-approximation's validity at intermediate energies; the close-coupling approximation, with its inclusion of back coupling and intermediate-state coupling, would seem to provide a more complete and realistic description of the collision process. A possible explanation is that at these energies the effect of electron exchange is comparable in magnitude but opposite in sign to the effect of back coupling and intermediate-state coupling; then the errors caused in the Born calculation by the neglect of both of these effects would partially cancel one another, yielding an intermediate-energy Born cross section of fortuitously high accuracy. The close-coupling calculation, by neglecting one effect but not the other, would be subject to greater error.

For the $4S$ and $4P$ states our experimental cross sections in the intermediate-energy range are 1.5 to 3 times smaller than the seven-state close-coupling values, which themselves are in

very good agreement with the Born-approximation results. This discrepancy is more serious than we found for the $3P$ and $3D$ states. It is a disagreement in shape as well as magnitude, and cannot be rectified simply by renormalizing our experimental results to the Born approximation at high energies.

The situation with the $4D$ state is similar to $3D$, in that the Born cross sections agree well with experimental values down to 15 eV, whereas the close-coupling cross sections appear to be too high. Full convergence of the close-coupling expansion may not have been reached since there is an appreciable difference between the results of the seven-state and eight-state calculations.

3. Low energy

Cross sections for $3P$ and $3D$ excitation, calculated by Moores and Norcross[50] by means of the four-state ($3S, 3P, 3D, 4S$) close-coupling approximation including exchange, are shown in Fig. 9. Considering first the $3P$ state, we see that at the lowest energies, i.e., from the $3P$ threshold at 2.1 eV up to 2.5 eV, our experimental cross section appears to be in good agreement with their calculations. However, the conclusiveness of this comparison is limited by our 0.75-eV energy resolution and by other experimental uncertainties that apply at these low beam energies, as discussed in Sec. III B. A more detailed and conclusive experimental verification of Moores and Norcross's $3P$ cross section in the immediate vicinity of threshold is afforded by Hafner's results.[32] The sudden decrease in slope we find in our experimental cross section at about 3 eV is indicated clearly, at 2.7–2.8 eV, by Moores and Norcross. At higher energies, i.e., 2.8 to 5 eV, there is a considerable discrepancy, in both shape and magnitude, between theory and experiment. The continuing rise with energy of the theoretical Q_{3P} at 5 eV conflicts with our experimental curve, which has a negligible slope at this point. Perhaps in this region, just below the ionization threshold, the close-coupling expansion may not be fully converged with only four states.

For the $3D$ state, Moores and Norcross's calculations cover only two impact energies, 4 and 5 eV. A comparison of theory and experiment is less conclusive for this state than for $3P$. Considerable uncertainty in the 4-eV experimental cross section arises from the finite-energy resolution in conjunction with the steepness of the excitation function, and from the rough estimates of the cascade from F levels (see Sec. IV B 7) at low energies. The experimental uncertainties at 5 eV are somewhat smaller, but the convergence of the close-coupling expression is probably less complete than it was for Q_{3P}. In view of these problems, the agreement within 25% of theory and experiment at 5 eV should be considered satisfactory, and even the much larger discrepancy at 4 eV should not be over interpreted.

4. Remarks concerning the accuracy of theoretical cross sections

While the overall agreement of the experimental cross sections at high energies with Born-approximation calculation is satisfactory, several observed trends for different families of states are puzzling. For instance, we find good agreement for all D states studied, but the Born cross sections are consistently 20–30% lower than the experimental values at high energies for the entire S family. For the P series the agreement is good for $3P$, but we find large discrepancy which varies in magnitude and sign among the higher members. One obvious question to raise about the accuracy of the Born-approximation calculation is the choice of the wave functions for the ground and excited states of the Na atom. Greene and Williamson[46] used Hartree-Fock-Slater wave functions, whereas in the calculation of Vainshtein, Opykhtin, and Presnyakov (second paper in Ref. 34) the atomic wave functions were determined semiempirically taking account of exchange. The part of the excited-state wave function which is most relevant for excitation cross section is in the region where it overlaps with the ground-state wave function. An excited-state wave function which reproduces well the energy is not necessarily adequate for cross-section calculation. In view of the lack of uniform accord between theory and experiment in the high-energy region for both Na and K, calculation of the Born cross sections using atomic wave functions that are more refined than the Hartree-Fock-Slater wave function is very desirable.

In the intermediate-energy region, the theoretical cross sections for $3P$ by the method of multistate close coupling agree well with experiment and show distinct improvement over the results of Born approximation. In fact, the success of the close-coupling calculation for the $3P$ state is quite impressive. However, this success is not duplicated for other states. Notably, the close-coupling cross sections for the $3D$ state are substantially larger than the experimental values. We mentioned the neglect of exchange between the incident and atomic electrons in the close-coupling calculation reported in Ref. 44 as a possible significant source of error. In addition, there is the long-standing question

of inclusion of continuum states in the close-coupling expansion when the incident energy exceeds the ionization limit of the target. Further theoretical work is needed to explore the utility of the method of close coupling for calculating excitation cross sections in the intermediate-energy region.

V. MEASUREMENTS OF POLARIZATION AND DETERMINATION OF THE DIRECT-EXCITATION CROSS SECTIONS OF THE SEPARATE ORBITAL MAGNETIC SUBSTATES OF $3P$

In this section we discuss our measurements of the polarization of electron-impact radiation emitted at right angles to the electron beam for several important transitions. We compare our results with those of other experimental and theoretical investigations, and then apply these results to obtain the direct-excitation functions for the separate magnetic substates of the $3P$ state.

The polarization was analyzed by means of a Polaroid filter (type HN-32 for visible radiation, type HNP'B for the uv, or type HR for the ir) situated several centimeters in front of the spectrometer entrance slit. The filter was manually oriented in one of two preset positions, transmitting light having its electric vector either parallel to or perpendicular to the electron beam. The intensities of these two components of the electron-impact radiation were measured relative to those of a standard, unpolarized source. Except in one instance this source was the tungsten strip lamp with a thin sheet of Teflon placed in front of the lamp window, an arrangement which was found in separate tests to produce negligible polarization. For the particularly important measurement of the $3P_{3/2}$-$3S_{1/2}$ polarization we used a different zero-polarization standard, namely, the electron-impact radiation of the companion line $3P_{1/2}$-$3S_{1/2}$. This light is taken to be rigorously unpolarized,[1] has the identical illumination pattern, and follows the identical optical path as the $3P_{3/2}$-$3S_{1/2}$ radiation; it was therefore thought to be the most reliable standard of unpolarized light. The various readings were taken in rapid succession and were repeated several times for each line at each energy. Photon counting was used for all polarization measurements, and the counting times were long enough so that statistical uncertainties in the polarization were a small fraction of a percent. The beam current was 2 to 10 μA. Our polarization data was taken at a number density of 3×10^{12} atoms/cm^3 for all transitions except $3P$-$3S$, for which the density was 2×10^{10} atoms/cm^3.

There are several sources of possible systematic error in our polarization measurements. One of these is the Hanle-effect depolarization caused by stray magnetic fields in the collision region. Such fields would include not only the uniform terrestrial field, but also nonuniform fields produced by the nearby Kovar window seals, spot welds, and various heater and filament currents (the heating coils had been wrapped in a bifilar configuration to hold these fields to a minimum). Because of the internal origin of some of these fields, external magnetic shielding did not seem appropriate. Instead, field nullification was achieved by externally applying a compensating field. The primary purpose was to eliminate curvature of the electron beam even at the lowest energies <3 eV; and, in fact, the straightness of the beam was our only *in situ* indicator of field nullification, since under experimental operating conditions the interior collision region was not accessible to a gaussmeter. The absence of beam curvature, as manifested visually and by the focusing properties of the electron gun, set an upper limit of about 200 mG on the transverse field in the collision region. A field of this magnitude would produce a Larmor precessional rate of the excited atoms of about $100°/\mu$s. A simple calculation shows that for the short-lived $3P$ and $3D$ states ($\tau=0.016$ and 0.020 μs) the polarization would be reduced by less than 1% of its value, which is below our limit of detection. For the longer-lived states, however, i.e., $4P$ and $5D$ ($\tau=0.125$ and 0.108 μs), the polarization could be reduced by a maximum of 25% of its value.

Another source of depolarization, which applies only to the $3P_{3/2}$-$3S_{1/2}$ line, is resonance-line scattering. We have held this to a minimum by taking our polarization data for this line at a low number density, approximately 2×10^{10} atoms/cm^3. At this density we estimate that fewer than 8% of the photons reaching the detector should have undergone resonance scattering while exciting the collision chamber; if we assume these scattered photons to be essentially unpolarized, then the effect of resonance scattering would be to reduce the polarization of the $3P_{3/2}$-$3S_{1/2}$ line by about 8% of its value—a small but not entirely negligible error. We have not corrected our data for this effect since our error estimate is simply an upper limit.

The depolarization resulting from the divergence of the electron beam (half-angle $\leq6°$) and of the detected radiation (half-angle $\leq3°$) was computed and found to be negligible in comparison with other effects.

It is to be noted that the above effects are all

of the depolarizing-type; hence, their result, if any, would be to decrease the magnitude of the measured polarization. The distortion of the shape of the polarization functions would probably be minimal, and the determination of the energy for which the polarization passes through zero would be unaffected.

A significant error in the polarization may occur immediately above threshold because of the steepness of the excitation functions in conjunction with the finite-energy spread of the electron beam.

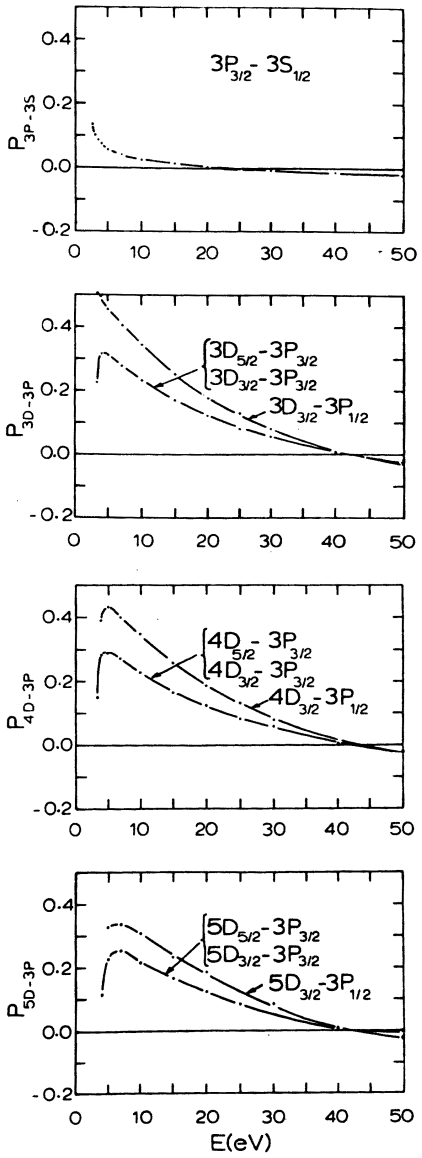

FIG. 10. Experimental polarization of separate components of $3P$-$3S$ and nD-$3P$ transitions. The splitting of the D levels is not resolved. The polarization of $3P_{1/2}$-$3S_{1/2}$, not shown, is zero.

A final source of error is the birefringence of the sapphire windows, although this was minimized by selecting windows with surfaces cut nearly perpendicular to the crystalline unique axis.

Our polarization data was taken at impact energies 2.5, 3, 3.5, 4, 5, 7, 10, 15, 20, 25, 30, 40, and 50 eV. The results for $3P_{3/2}$-$3S_{1/2}$ and for both components of the $3D$-$3P$, $4D$-$3P$, and $5D$-$3P$ doublets are shown in Fig. 10. (In the convention used the polarization is considered positive if the electric vector is parallel to the electron beam.) In addition to these results, polarization measurements of $3P_{1/2}$-$3S_{1/2}$, $5S$-$3P$, $6D$-$3P$, and $4P$-$3S$ were also made. The first two of these were found to be unpolarized in accordance with theory. The $6D$-$3P$ polarization, measured only at 6.5 eV, is noticeably less than that of $5D$-$3P$. The $4P$-$3S$ polarization function resembles that of $3P$-$3S$, but is smaller and subject to considerably greater uncertainty.

An instructive comparison of the $3P$-$3S$ and $3D$-$3P$ polarization functions of sodium with their counterparts in potassium can be made by examining, in turn, Fig. 10 of the present work and Fig. 11 of Ref. 5. Looking first at the resonance transition we see that the $3P_{3/2}$-$3S_{1/2}$ line of Na is less polarized than the $4P_{3/2}$-$4S_{1/2}$ line of K. This is evidently a consequence of the fact that the hyperfine splitting of the $3P_{3/2}$ state of ^{23}Na is approximately three times larger than that of the $4P_{3/2}$ state of ^{39}K,[19] permitting more extensive depolarization by the $J \cdot I$ coupling. We also see from these curves that the $3P_{3/2}$-$3S_{1/2}$ polarization function of Na passes through zero at a somewhat higher energy, 22.5 ± 1 eV, than does that of the $4P_{3/2}$-$4S_{1/2}$ line of K, 17 ± 1 eV. For each element the impact energy for unpolarized resonance radiation is equal to about 10.6 times the threshold energy, i.e., 2.10 eV for the $3P$ level of Na, 1.61 eV for the $4P$ level of K. Similarly, the leading members of the diffuse series of the two atoms are unpolarized at the same impact energies as each other when measured in units of their respective $3D$ threshold energies. Specifically, the Na $3D$-$3P$ transition is unpolarized at 41 ± 1 eV, or 11.3 times the Na $3D$ threshold energy, 3.61 eV, while the K $3D$-$4P$ transition is unpolarized at 31 ± 1 eV, or 11.6 times the K $3D$ threshold energy, 2.67 eV.

Continuing the comparison, we find that the $3D$-$3P$ transition in Na is more strongly polarized than $3D$-$4P$ in K. This may be a result of the smaller hfs[19,51] and shorter radiative lifetime[18] of the $3D$ state of Na relative to those of K. [Data available in the literature concerning the extremely small hfs of D states of Na and K are

fragmentary and, in fact, include no measurements for the $3D$ states. However, from the data for other nD states summarized by Arimondo *et al.*,[19] along with the scaling law demonstrated in the review by Happer,[51] i.e., that for a given isotope the hyperfine coupling constants of members of a sequence of states having the same L and J, but different n, are proportional to $(n^*_{nL})^{-3}$—we can make fair estimates of the hfs of the $3D$ states of both Na and K. In this way we find that the hfs of the $3D$ and higher D states of Na are smaller than, or at most comparable to, the natural radiative widths of the states, while for K the D-state hfs are comparable to the natural widths.]

Examining our diffuse series polarization data we find that for both Na and K the combined $(nD_{5/2}\text{-}3P_{3/2}+nD_{3/2}\text{-}3P_{3/2})$ lines, which we abbreviate as $D\text{-}P_{3/2}$, are polarized less than the $nD_{3/2}\text{-}3P_{1/2}$ line, abbreviated $D\text{-}P_{1/2}$. A theoretical relation between the polarizations of the two components,

$$P_{D-P_{3/2}} = 16P_{D-P_{1/2}}/(25 - 3P_{D-P_{1/2}}), \tag{7}$$

can be derived from the Oppenheimer-Penney theory,[52] neglecting hfs, with the aid of standard LS coupling formulas.[53] This equation fits our Na data very well, except perhaps at low energies. The fit to our K data is not quite so close, reflecting perhaps the larger hfs of the $3D$ state of K.

Above about 15 eV the polarization functions of the $3D\text{-}3P$, $4D\text{-}3P$, and $5D\text{-}3P$ doublets of Na have a very regular behavior and resemble each other closely. Differences develop at lower energies, however. We see that the polarization at low energies is depressed by increasing amounts as n is increased from 3 to 5, and the trend continues for $n=6$ (not shown). As the impact energy is decreased below 10 eV the $nD\text{-}3P$ polarization functions rise to a maximum then drop towards zero upon closer approach to threshold. Such behavior has previously been observed for the unresolved $5D\text{-}3P$ doublet of sodium[31] and the $3D\text{-}2P$ doublet of lithium,[54] as well as in other elements. It is termed anomalous as it appears to indicate a threshold polarization value that is much smaller than predicted by the established theory.[52] The theoretical calculation, which depends essentially upon the conservation of angular momentum and upon conventional angular-momentum-coupling theory—but not upon any specific collision theory—yields comparatively large threshold polarization values of 0.600 for the $D\text{-}P_{1/2}$ line, 0.414 for the $D\text{-}P_{3/2}$ lines, or 0.479 for the combined $D\text{-}P$ transition. (The calculation neglects hfs, as justified earlier.) Our experimental results, as illustrated in Fig. 10, do not appear to agree with these predictions, yet it cannot be concluded that they are in direct conflict, since the theoretical values apply only in the limit, as threshold is approached, whereas our lowest-energy data begins a fraction of a volt above threshold. Our experimental curves cannot reliably be extrapolated back to threshold owing to the possibility of irregular behavior there. Heideman, van de Water, and van Moergestel[55] have recently offered an interpretation of anomalous threshold polarization that resolves the apparent conflict between theory and experiment. They suggest that, beginning at energies immediately beyond threshold, there exist correlations between the motions of the projectile and valence electrons that persist out to large distances from the nucleus, and are therefore associated high values of M_L (component of orbital angular momentum along electron beam axis) even though the kinetic energy of the recoiling electron is very small.

At energies arbitrarily close to threshold, only the $M_L=0$ substates can be excited as dictated by conservation of angular momentum; there the polarization would approach its maximum value given correctly by conventional theory. But with only a slight increase in energy, a spectrum of M_L substates would be excited causing a sudden depression of the polarization. The polarization could fall quickly to a relative minimum, then rise more gradually as energy is increased further, and resume its normal behavior. If the minimum were deep enough and close enough to threshold, then the true threshold polarization would not be apparent to the experimenter employing an electron beam of finite-energy resolution; it would instead appear that the polarization function approached zero as the impact energy approached threshold. In less extreme cases, the apparent effect would be a polarization function that, starting at its maximum value at threshold, fell rapidly with a small increase in energy, then continued to fall more gradually at higher energies. Heideman *et al.* expect this effect to be greater for excitation of the higher n or L states because they are spatially more extended. The higher-L states also offer a larger spectrum of M_L values to further enhance the effect.

Our data provides some support for this interpretation of anomalous polarization. For the relatively compact $3P$ state the only manifestation is a steep drop following threshold. For the D states the anomalous behavior is more pronounced; the reduction in polarization and the

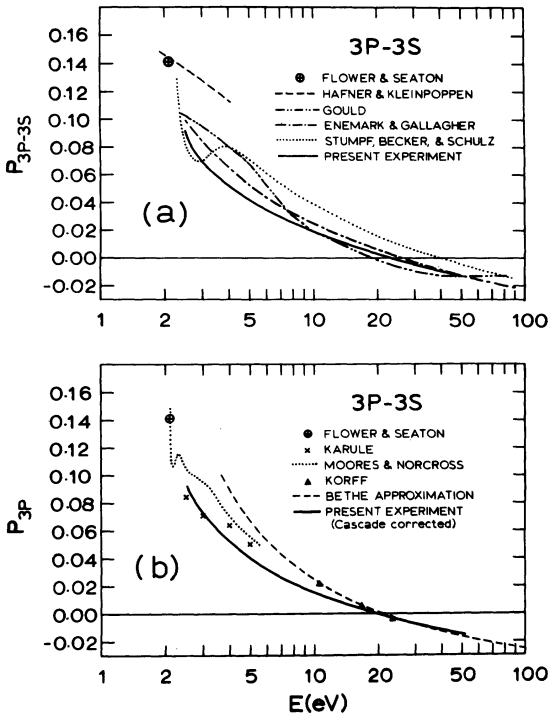

FIG. 11. Polarization of combined $3P$-$3S$ doublet. (a) Comparison of our results, uncorrected for cascade, with those of other experiments, (b) comparison of our results, corrected for cascade, with various theoretical calculations.

range of energies over which it extends increases with n. At energies above 15 eV, where the correlation of motion would be small, the polarization functions resume their normal, monotonic decline. It is interesting to note that if we try to eliminate the correlation effect from these curves by making plausible, smooth extrapolations of them from the portion beyond 15 eV back to the thresholds, then we obtain threshold polarization values comparable to those predicted by conventional threshold theory, as given earlier.

Previous experimental measurements and theoretical calculations of the polarization of Na electron-impact radiation have been limited primarily to the $3P$-$3S$ transition. Most of these refer to the combined doublet, so to facilitate comparisons we have converted our separate component data to combined doublet data, making use of the relation

$$P_{3P-3S} = 6P_{3P_{3/2}-3S_{1/2}}/(9 - P_{3P_{3/2}-3S_{1/2}}), \qquad (8)$$

in which it is implicit that the $3P_{1/2}$-$3S_{1/2}$ component is unpolarized, and that the ratio of the optical-excitation cross sections of the two components is 2:1.

Figure 11(a) contains all the experimental results. Except for ours, these experiments are of the crossed-beam-type, with energy resolutions ranging from 0.2 to 0.5 eV. The threshold value 0.141, computed by Flower and Seaton,[56] using the theory of Percival and Seaton, is also included in Fig. 11(a) as a point of reference. Our data cannot be considered to confirm or conflict with this value for reasons already discussed. It is clear from this figure that over the entire energy range our result is consistent only with that of Enemark and Gallagher,[3] from which it differs by less than 0.010 except in the neighborhood of 3.5 eV, where the difference reaches 0.015. Even these differences approach the maximum that we would think attributable to our experimental uncertainties and they exceed the uncertainties assigned by Enemark and Gallagher.

Among these various experimental results, only those of Hafner and Kleinpoppen[54] show a smooth, unambiguous approach to the theoretical threshold value. The large discrepancy between their results and ours is puzzling. The polarization function of Gould[31] has a very different shape from ours, which is also difficult to account for. At about 40 eV his curve ceases to decline and holds a constant value up to the high-energy limit of his experiment. This is similar to the behavior of his optical-excitation functions which we have commented on in Sec. III C. More recently Stumpf, Becker, and Schulz[33] have measured the polarization of the separate $3P$-$3S$ components which we have combined together for presentation in Fig. 11(a) by applying Eq. (8). (The curve shown here is our own smoothed-out interpretation of Stumpf, Becker, and Schulz's results, which in their original presentation consisted of a large number of individual data points with associated error bars.) The structure of this curve in the vicinity of threshold, i.e., the steep descent and the relative minimum, is interesting in light of our earlier discussion of threshold anomalies. Our own curve has a much simpler shape, but in view of the 0.5-eV intervals between our data points and the 0.75-eV width of our beam, it is possible that some details of structure could have gone undetected by our experiment. Above about 4 eV the curve of Stumpf, Becker, and Schulz is similar to ours in shape but lies consistently higher. The energy at the zero-crossing point, 40 eV, seems improbably high.

In Fig. 11(b) we collate a number of results of collision-theory calculations, all of which incorporate the analysis of Flower and Seaton in

order to make the necessary connection between the electron-impact process and the subsequent radiative decay process. None of these calculations includes the contribution of radiative cascade into $3P$ from S and D states. Thus they are to be interpreted as giving the polarization of that portion (typically 80–90%) of the $3P$-$3S$ radiation that results from the direct excitation of the $3P$ alone. We denote this quantity by P_{3P} to distinguish it from P_{3P-3S} which includes cascade contributions. By correcting our experimental P_{3P-3S} for cascade, we have obtained an experimental P_{3P} which is plotted in Fig. 11(b). The corrections were small (≤ 0.003, which is less than our overall experimental uncertainty) and their main effect was to shift the zero-crossing point from 22.5 eV down to about 20.5 eV.

Included in Fig. 11(b) along with our results are the threshold value of Flower and Seaton and three close-coupling results, namely, the two-state result by Karule,[57] the seven-state result by Korff,[58] and the four-state result by Moores and Norcross.[50] Also included is a Bethe-approximation calculation which is based upon the theory developed by McFarlane[59] as applied by Heddle.[60] In this approximation P_{3P} can be computed as a function of impact energy E according to

$$P_{3P}=P_0[3-\ln(E/E_0)][P_0+(2-P_0)\ln(E/E_0)]^{-1}, \quad (9)$$

where P_0 is the threshold polarization given as 0.141 by Flower and Seaton, and E_0 is a parameter to be derived from a Fano plot of the Born- or Bethe-approximation calculation of Q_{3P}. From Vainshtein's[34] Born calculations for Q_{3P} we obtain $E_0=1.046$ eV. Substitution of these values of E_0 and P_0 into Eq. (9) yields the Bethe approximation of P_{3P} shown in Fig. 11(b).

An examination of Fig. 11(b) shows that our experimental P_{3P} is smaller than most of the theoretical values. Our results clearly disagree with the Bethe approximation below 10 eV and agree only marginally with the calculation by Moores and Norcross. Above about 15 eV, however, there is something of a consensus among our experimental results, the Bethe approximation, and the seven-state close-coupling calculation of Korff. There is excellent agreement on the zero-polarization energy 20.5 ± 1 eV, or 9.7 threshold units for the cascade-free polarization function.

From our measurements of the optical-excitation functions and polarization functions for the $3P$-$3S$, nS-$3P$, and nD-$3P$ transitions, we can determine the direct-excitation functions for the individual orbital magnetic substates $|M_L, M_S\rangle$ of the $3P$ state. Because the incident electrons and the target atoms were initially unpolarized, the substate cross sections are symmetric in

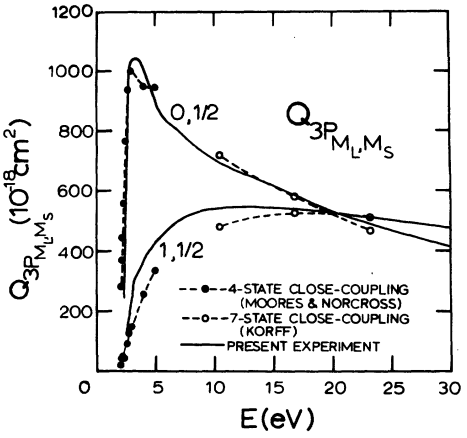

FIG. 12. Experimental direct-excitation functions of magnetic substates of the $3P$ state. Cross sections are symmetric in M_L and M_S, so that $Q_{3P}=2Q_{^3P_{0,1/2}}+4Q_{^3P_{1,1/2}}$.

M_L and in M_S. Thus, we need solve only for the $|M_L,M_S\rangle=|0,\frac{1}{2}\rangle$ and $|1,\frac{1}{2}\rangle$ cross sections, which are related to the total direct $3P$ cross section by

$$Q_{3P}=\sum_{M_L,M_S} Q_{^3P_{M_L,M_S}}=2Q_{^3P_{0,1/2}}+4Q_{^3P_{1,1/2}}. \quad (10)$$

The procedure for determining the substate cross sections has been described in Sec. VI of Ref. 5. They can easily be expressed in terms of the cascade-corrected cross section Q_{3P} and polarization function P_{3P} by[56]

$$Q_{^3P_{0,1/2}}=\frac{Q_{3P}}{6}\left(1+\frac{2K_{3P}P_{3P}}{3-P_{3P}}\right),$$
$$Q_{^3P_{1,1/2}}=\frac{Q_{3P}}{6}\left(1-\frac{K_{3P}P_{3P}}{3-P_{3P}}\right). \quad (11)$$

Here K_{3P} is a constant which depends on the hfs and the natural radiation width of the $3P_{3/2}$ state and is equal to 20.18. [Expressed in the notation of Flower and Seaton, K_{3P} is written as $12/(9\alpha-2)$, where $\alpha=0.2883$.]

The $3P$ magnetic substate cross sections derived from our experimental measurements are shown in Fig. 12. Like the corresponding data for potassium,[5] these results show explicitly that near threshold the $M_L=0$ substates are strongly excited, and that all the substates are equally excited at the zero-polarization energy, 20.5 eV. At higher energies the excitation favors $M_L=\pm 1$ substates. Also shown in Fig. 12 are the results of Moores and Norcross at low energies, and those of Korff at intermediate energies, which can be derived from Figs. 9 and 11 along with Eq. (11). The extent of agreement of both of these theoretical results with our experiment is satis-

factory, when account is taken of the sensitivity of our experimental substate cross sections to small errors in the measured polarization.

Note added in proof. We are advised by B. Stumpf that the $3P$-$3S$ polarization function has been remeasured by Stumpf, Becker, and Schulz, and that the new results are typically 0.012 lower than the original. A paper covering this work is forthcoming.

ACKNOWLEDGMENT

The authors wish to acknowledge support by the Air Force Office of Scientific Research.

[1]B. L. Moiseiwitsch and S. J. Smith, Rev. Mod. Phys. 40, 238 (1968). Note erratum concerning polarization in Rev. Mod. Phys. 41, 574 (1969).
[2]B. H. Bransden and M. R. C. McDowell, Phys. Lett. C 30, 207 (1977); 46, 249 (1978).
[3]E. A. Enemark and A. Gallagher, Phys. Rev. A 6, 192 (1972).
[4]I. P. Zapesochnyi, E. N. Postoi, and I. S. Aleksakhin, Zh. Eksp. Teor. Fiz. 68, 1724 (1975) [Sov. Phys.—JETP 41, 865 (1975)].
[5]J. O. Phelps, J. E. Solomon, D. F. Korff, C. C. Lin, and E. T. P. Lee, Phys. Rev. A 20, 1418 (1979).
[6]A. V. Phelps, Ann. Geophys. 28, 611 (1972).
[7]Available from Optronics Laboratories, Inc., 7676 Fenton St., Silver Spring, Md. 20910.
[8]Available from Corion Instrument Corp., 77 Jeffrey Ave., Holliston, Mass. 01746.
[9]S. F. Pellicori, Appl. Opt. 3, 361 (1964).
[10]M. Kasha, J. Opt. Soc. Am. 38, 929 (1948).
[11]H. L. J. Backstrom, Naturwissenschaften 13, 251 (1933).
[12]C. M. Penchina, Appl. Opt. 6, 1029 (1967).
[13]R. E. Poulson, Appl. Opt. 3, 99 (1964).
[14]R. Hultgren, P. D. Desai, D. T. Hawkins, M. Gleiser, K. K. Kelley, and D. D. Wagman, *Selected Values of the Thermodynamic Properties of the Elements* (American Society for Metals, Cleveland, 1973).
[15]*Smithsonian Physical Tables*, edited by F. E. Fowle (Smithsonian Institution, Washington, D. C., 1954).
[16]I. P. Zapesochnyi and L. L. Shimon, Opt. Spektrosk. 5, 621 (1962) [Opt. Spectrosc. (USSR) 5, 355 (1962)].
[17]L. M. Volkova, Opt. Spektrosk. 11, 755 (1961) [Opt. Spectrosc. (USSR) 11, 420 (1961)].
[18]W. L. Wiese, M. W. Smith, and B. M. Miles, *Atomic Transition Probabilities*, U. S. National Bureau of Standards, Reference Data Series—22 (U. S. Government Printing Office, Washington, D. C., 1969), Vol. II.
[19]E. Arimondo, M. Inguscio, and P. Violino, Rev. Mod. Phys. 49, 31 (1977).
[20]A. N. Nesmeyanov, *Vapor Pressure of the Chemical Elements* (Academic, New York, 1963).
[21]M. Hugon, F. Gounand, and P. R. Fournier, J. Phys. B 13, L109 (1980).
[22]T. F. Gallagher, S. A. Edelstein, and R. M. Hill, Phys. Rev. A 15, 1945 (1977).
[23]T. F. Gallagher and W. E. Cooke, Phys. Rev. A 19, 2161 (1979).
[24]T. F. Gallagher, S. A. Edelstein, and R. M. Hill, Phys. Rev. A 11, 1504 (1975).
[25]T. F. Gallagher, S. A. Edelstein, and R. M. Hill, Phys. Rev. A 14, 2360 (1976).
[26]T. F. Gallagher and W. E. Cooke, Phys. Rev. Lett. 42, 835 (1979).
[27]G. Haft, Z. Phys. 82, 73 (1933).
[28]W. Christoph, Ann. Phys. (Leipzig) 23, 51 (1935).
[29]I. P. Zapesochnyi and L. L. Shimon, Opt. Spektrosk. 19, 480 (1965) [Opt. Spectrosc. (USSR) 19, 268 (1965)].
[30]I. P. Zapesochnyi and O. B. Shpenik, Zh. Eksp. Teor. Fiz. 50, 890 (1966) [Sov. Phys.—JETP 23, 592 (1966)].
[31]G. N. Gould, Ph.D. thesis, University of New South Wales, 1970 (unpublished).
[32]H. Hafner, Phys. Lett. A 43, 275 (1973).
[33]B. Stumpf, K. Becker, and G. Schulz, J. Phys. B 11, L639 (1978).
[34]L. A. Vainshtein, V. Opykhtin, and L. Presnyakov, P. N. Lebedev Institute of Physics Report No. A-53 (unpublished); Zh. Eksp. Teor. Fiz. 47, 2306 (1964) [Sov. Phys.—JETP 20, 1542 (1965)]. Results summarized in Ref. 1.
[35]M. Inokuti, Rev. Mod. Phys. 43, 297 (1971).
[36]A. Lindgard and S. E. Nielsen, At. Data Nucl. Data Tables 19, 533 (1977).
[37]E. M. Anderson and V. A. Zilitis, Opt. Spektrosk. 16, 177 (1964) [Opt. Spectrosc. (USSR) 16, 99 (1964)].
[38]E. Biemont and N. Grevesse, At. Data Nucl. Data Tables 12, 217 (1973).
[39]D. Kaiser, Phys. Lett. A 51, 375 (1975).
[40]C. M. Huang and C. C. Wang, Phys. Rev. Lett. 46, 1195 (1981).
[41]I. P. Zapesochnyi, Teplofiz. Vys. Temp. 5, 7 (1967) [High Temp. (USSR) 5, 6 (1967)].
[42]S. J. Buckman and P. J. O. Teubner, J. Phys. B 12, 1741 (1979).
[43]S. K. Srivastava and L. Vuskovic, J. Phys. B 13, 2633 (1980).
[44]D. F. Korff, S. Chung, and C. C. Lin, Phys. Rev. A 7, 545 (1973).
[45]M. M. Felden and M. A. Felden, J. Opt. Soc. Am. 51, 1709 (1973).
[46]T. J. Greene and W. Williamson, Jr., At. Data Nucl. Data Tables 14, 161 (1974).
[47]E. Clementi and C. Roetti, At. Data Nucl. Data Tables 14, 177 (1974).
[48]K. Omidvar, Phys. Rev. 133, A970 (1964). The $1s \rightarrow 2p$ excitation data are reviewed in Ref. 1.
[49]S. Chung and C. C. Lin, Phys. Rev. A 17, 1874 (1978).
[50]D. L. Moores and D. W. Norcross, J. Phys. B 5, 1482 (1972).
[51]W. Happer, in *Proceedings of the Fourth International Conference on Atomic Physics*, edited by G. zu Putlitz, E. W. Weber, and A. Winnacker (Plenum, New York, 1975), p. 651.
[52]I. C. Percival and M. J. Seaton, Philos. Trans. R. Soc. London Ser. A 251, 113 (1958).
[53]E. U. Condon and G. H. Shortley, *The Theory of Atomic Spectra* (Cambridge University Press, Cambridge, England, 1970).
[54]H. Hafner and H. Kleinpoppen, Z. Phys. 198, 315

(1967).
[55]H. G. M. Heideman, W. van de Water, and L. J. M. van Moergestel, J. Phys. B 13, 2801 (1980).
[56]D. R. Flower and M. J. Seaton, Proc. Phys. Soc. London 91, 59 (1967).
[57]E. Karule, J. Phys. B 3, 860 (1970).
[58]D. F. Korff, Ph.D. thesis, University of Wisconsin, 1973 (unpublished).
[59]S. C. McFarlane, J. Phys. B 7, 1756 (1974).
[60]D. W. O. Heddle, J. Phys. B 12, 489 (1979).